POLITECNICO DI TORINO

Laurea Magistrale in Ingegneria Civile

Effectiveness of Rejuvenating Agents for reclaimed asphalt through the evaluation of the model system

Relatore

Prof. Ezio Santagata

Correlatori

Prof. Davide Dalmazzo

Prof. Pier Paolo Riviera

Ing. Leonardo Urbano

Candidato

Carolina Gil Botero

ABSTRACT

Reclaimed Asphalt (RA) represents the material obtained from the milling and crushing of old and damaged asphalt mixture employed in the construction of the flexible pavement. The recycling of RA in new asphalt mixture has become attractive thanks to its technical, economic, and environmental advantages. In fact, RA recycling leads to a reduction of costs, providing a contextual solution to disposal problems and the minimization of environmental footprint. However, when the recycling of RA exceeds a limiting amount (normally more than 50%), the final mixture will be characterized by poor performance tightly connected with the presence of the aged binder in RA. Thus, to properly maximize recycling, the use of Rejuvenating Agents is required to restore the chemical and rheological properties of the aged and stiff RA bitumen.

Actually, there are not any standards for the evaluation of the effectiveness of the Rejuvenating Agents and their principal effects related to the selection of the dosage and its diffusion in the binder matrix. Two alternative approaches can be followed to investigate the effectiveness of such additives. The first is based on the chemical and rheological analysis of extracted binder from RA, adequately mixed with Rejuvenating Agents: this procedure requires the use of solvents that can damage the extracted binder. The second approach studies bituminous mixtures containing the rejuvenated RA: nevertheless, this procedure is time and money consuming. Although both methodologies have an important confirmation in the scientific literature, some concerns are still present. To overcome such disadvantages, a new approach to evaluate the effectiveness of the Rejuvenating Agents based on a Model System (MS) was developed in the Road Materials Laboratory of Politecnico di Torino.

The Model System is constituted by a single-sized 5/8 RA material, selected to limit the presence of the finer fractions and RA cluster, ensuring the same granular composition for each

MS. MS was designed to obtain a constant value of the Voids in the Mineral Aggregate (VMA) to have a constant lithic structure and similar contact points between aggregates. Therefore, the mechanical behaviour of MS depends mainly on the binder phase, limiting the effect of aggregates interlocking. The VMA target selected is equal to 30%.

The objective of the present work is to validate the previous investigations on the Model System using three different RA sources, combined with two different Rejuvenating Agents, in order to assess the possible dependency of the rejuvenating effect on RA. It is important to highlight that RA of each source has a different origin, age, gradation, bitumen type, among others.

Regardless of RA source, three different MS were prepared: (i) a black system made with 100% 5/8 RA; (ii) a rejuvenated system composed of 5/8 RA mixed with a Rejuvenating Agent; (iii) a white system constituted by the aggregates extracted from RA mixed with 50/70 neat binder, keeping constant the percentage of the binder characteristic of each 5/8 RA source. Once the optimal dosage was defined considering the linear viscoelastic behaviour, the indirect tensile strength test was performed to study the performance at low temperatures.

INDEX

1. INTRODUCTION

Hot mix asphalt (HMA) is the most widely used paving material worldwide. When flexible pavements reach the end of their service life, removing, milling, and crushing are realized, but this Reclaimed Asphalt (RA) is still valuable. The milled materials can be reused, lowering the virgin material required in new constructions. RA recycling in new asphalt mixture has become attractive thanks to its technical, economic, and environmental advantages. In fact, RA recycling leads to a reduction of costs, providing a contextual solution to disposal problems and the minimization of environmental footprint. However, RA is composed of aggregates and aged bitumen; this altered binder has rheological and mechanical properties different from virgin bitumen.

Implementing high content of RA in a Hot Mix Asphalt requires a new mixture design that ensures that a poor performance will not characterize the final pavement because of the aged binder in RA. Thus, to properly maximize recycling, the use of Rejuvenating Agents is required to restore the rheological properties of the recycled, oxidized, volatilized, polymerized, aged binder. This solvent transforms the stiff binder properties close to the virgin binder ones, making it possible to increase the content of RA in a considerable amount.

Hence, there are new tasks to investigate, as the interaction effect of Rejuvenating Agents and RA, the definition of the optimum dosage, and the response of the final mixture. There are two methodologies to aboard the study of these solvents and the aged binder in the literature. The first one realizes the extraction of the aged bitumen from RA and executes the rheological analysis. The second approach is based on the direct analysis of the bituminous mixture containing regenerated milled material. Nevertheless, both methodologies have many

considerations that must be evaluated. The first methodology requires the usage of solvents that can damage the binder extracted, changing its properties; they also can be harmful to operators and the environment. In contrast, the second methodology involves arduous investigation techniques and methods, even though it reproduces the more reliable results closer to reality.

The University Politecnico di Torino developed a new approach to evaluate the Rejuvenating Agents' effectiveness through the Model System (MS) that overcome such disadvantages. The objective of the present work is to validate the previous investigations on the Model System using three different RA sources, combined with two different Rejuvenating Agents, in order to assess the possible dependency of the rejuvenating effect on RA.

MS is based on three main parameters. The first one defines that the material to study corresponds to a single-sized 5/8 RA. This constraint avoids the inclusion of fine particles characterized by having a different binder film thickness and the addition of clusters that have an unknown composition. The second parameter establishes that it is required to work with a target value of Voids in Mineral Aggregates (VMA), guaranteeing that all samples have the same lithic structure independently of the binder phase-type. Finally, the last consideration evaluates the VMA target equal to 30%; therefore, having a lithic structure with high content of air voids and limited contact points, the mechanical behaviour of MS depends mainly on the binder phase, limiting the aggregate performance. Furthermore, following the above parameters allows the interlocking effect between aggregates and the shape and granulometry distribution differences to be limited. Nevertheless, it must be highlighted that MS does not reproduce the mechanical behaviour of bituminous mixtures made up of 100% RA.

The present thesis is organized into six chapters, including the theoretical framework, materials properties and composition, testing methodology, presentation of results, and conclusions.

1.1 OBJECTIVES

The main objective of the present work is to validate the previous investigations on the Model System using different RA sources, combined with distinct Rejuvenating Agents, in order to assess the possible dependency of the rejuvenating effect on RA. Three model systems have been evaluated:

- A black system (BS) constituted by 100% 5/8 RA;
- A rejuvenated system (RS) composed of 100% 5/8 RA mixed with the Rejuvenating Agent (E or P);
- A white system (WS) constituted by the aggregates extracted from RA mixed with 50/70 neat binder, keeping constant the percentage of the binder characteristic of each 5/8 RA source. This MS was introduced as a reference condition to evaluate the regenerating action of additives E and P.

First, it was required to define the optimal dosage of Rejuvenating Agents for each material source, analyzing its linear viscoelastic response. Then the sample specimens were tested to determine the mechanical properties and understand the behaviour of each condition and the effectiveness of the Rejuvenating Agent. The tests developed were Indirect Tensile Stiffness Modulus, Indirect Tensile Strength, and Dynamic Modulus.

Other objectives of the present work include:

- Using the results obtained, analyze how RA's workability, stiffness, and strength change in function of the addition of the Rejuvenating Agents.
- It is required to examine the ageing stage of each material source, comparing the properties between the Black and White system of each source.
- Analyze the possibility of interchanging advanced test methodologies with less expensive and more reachable approaches.

2. THEORETICAL FRAMEWORK

The bituminous mixtures are the material employed in the construction of flexible road pavements. Once the pavement reaches the ultimate condition of its service life, such materials are removed by milling procedure and, as a result, the Reclaimed Asphalt (RA) is obtained. While in the past, RA was disposed of entirely in landfills, nowadays, RA is considered a precious resource that can be valorized to obtain new mixtures with superior environmental and economic properties. Therefore, RA is generally recycled through hot or cold recycling technology depending on the desired properties and design pavement layer.

Nevertheless, it is necessary to fully characterize RA materials, mainly when it is recycled for new Hot Mix Asphalt. This section of the present work reviews the existing literature on the materials analyzed in this study, RA and Rejuvenating Agents.

In 1970, some attempts were carried out to recycle RA due to the energetic crisis that led to a dramatic increase in the price of the petroleum products, such as bituminous binder. Since then, the investigations and technologies based on this recycling strategy have started to grow (Moghaddam & Baaj, 2016). From that time, the benefits of RA in the new HMA have been noticeable, such as the cost reduction and minimization of environmental footprint by cutting emissions, fuel usage, and the non-renewable resources demand (Moghaddam & Baaj, 2016). Other benefits are the diminution of the required binder, minimization of the scarcity of quality material and waste production, helping with disposal problems. Additionally, mixtures containing RA Provide stronger moisture resistance than virgin HMA since aggregates are already covered and protected with a binder film.

The cost reduction obtained when implementing RA in the mix design can reach 14 to 34% for RA content between 20 and 50% (Kendhal & Mallick, 1997). The following picture shows a cost analysis by implementing different percentages of RA (0-100%). Results are consistent with previous studies.

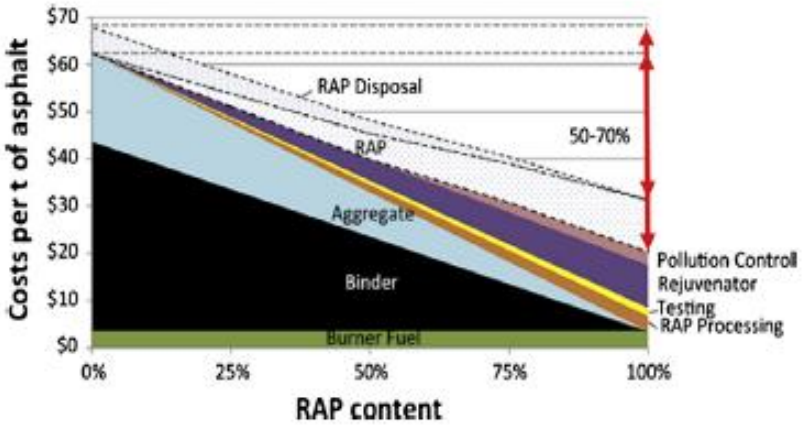

Figure 1. Costs of materials in hot mix recycling. (Moghaddam & Baaj, 2016)

Despite the advancements in the design of HMA containing RA, authorities still have many restrictions to avoid durability problems, and premature distresses as fatigue and low-Temperature cracking related to the aged binder included in RA. They limited RA content because only for a small percentage (less than 20%), the aged binder will not affect blending properties (Al-Qadi, Elseifi, & Carpenter, 2007). Therefore, the main objective is to ensure confidence in the design procedure and address the durability concerns, increasing RA percentage included in the HMA mix design, avoiding a lower life and incrementing maintenance costs, energy consumption and emissions.

2.1 RECLAIMED ASPHALT (RA)

The reclaimed asphalt (RA) is the processed site-won asphalt, suitable and ready to be used as a constituent material for asphalt mixture, after being tested, assessed, and classified, as defined

by the EN 13108-8 (2016). Some methods to incorporate RA includes Hot recycling at the asphalt plant, Hot in-place recycling, Cold-in-place recycling and Full-depth reclamation (Moghaddam & Baaj, 2016). This material is characterized by a stiff, dry, and brittle binder that, because of the ageing process, the Maltenes/Asphaltenes ratio is reduced.

RA influences new mixtures' volumetric properties and performance, mainly when a high amount of RA is used. Apart from aggregate-asphalt interactions in the old pavement, these properties depend on RA milling and crushing processes. Therefore, physical and consensus RA aggregate and binder properties need to be obtained before being used to construct a new pavement structure (Moghaddam & Baaj, 2016).

Therefore, it is also essential to understand the interaction between aged and virgin asphalt binders in RA. Three different possible cases may characterize it:

1. Black Rock, if RA has no interaction, it behaves as an aggregate since the bitumen film that covers the aggregates of the aged milled material is entirely inert. Therefore, there are no changes in virgin asphalt properties.
2. Partial Blending, if just part of the aged bitumen present in RA is mixed with the virgin binder, obtaining a bitumen film that has mechanical characteristics in between those of the virgin and aged material. The non-rejuvenated part will remain inert.
3. Total Blending, if aged asphalt, totally blends with a virgin binder during mixing. Many design procedures assume this condition, as the aged binder is fully available in the mixture and would effectively contribute to the blend. However, the amount of virgin asphalt binder can be reduced by the total amount of asphalt binder in RA and will have uniform mechanical characteristics.

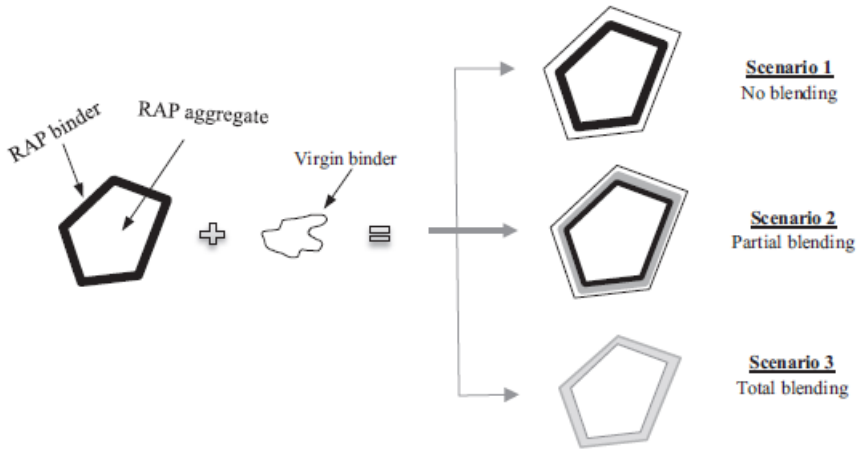

Figure 2. RA binder and virgin binder blending scenarios. (Moghaddam & Baaj, 2016)

The Designer must assume one of those three cases. However, if it is supposed that the material totally blends when it behaves like black rock, then the binder will not be stiff enough, and insufficient asphalt binder is used. In contrast, it is assumed that RA does not blend with virgin asphalt binder when is blending, then the binder will be stiffer than expected, and a rich mix will result.

2.2 REJUVENATING AGENT

soft binder and softening agents or Rejuvenating Agents may be included To restore the rheological properties. Softening agents can be used when a lower amount of RA is used; it lowers the viscosity of the aged binder and reduces the amount of RA. In contrast, the Rejuvenating Agent restores RA's physical and chemical properties. Rejuvenating Agents are lubricating and extender oils. They control the syneresis, reduce the stiffness and viscosity but increase ductility (Al-Qadi, Elseifi, & Carpenter, 2007). Furthermore, they are suitable for either highly oxidized mixtures or mixtures containing a high percentage of RA (more than 25% RA) or recycled asphalt shingles (RAS) (Moghaddam & Baaj, 2016). Types of

Rejuvenating Agents include plant oils, waste-derived oils, engineered products, and traditional and non-traditional refinery base oils.

In literature can be found three rejuvenating methods; the first one is to mix them with aged asphalt mixture at high temperature (140ºC - 150ºC) or spray it into the surface. The second one is the Rejuvenator sela material (RSM), typically used after four years of pavement construction; it can improve mixture properties against moisture, gasoline, diesel, weathering, improve crack development, and prevent binder oxidation, penetrating the voids. However, it must penetrate the required depth because it might reduce skid resistance; also, it can be harmful to the environment. The third possible procedure is the encapsulation process; in this method, a Rejuvenating Agent is contained in capsules that degrades from applied traffic loads through the years (Moghaddam & Baaj, 2016).

The rejuvenating process can be studied as Carpenter and Wolosick (1980), using a two-staged extraction method, considering the inner and outer layers separately. The rejuvenation process starts with a low viscosity layer around the aggregates coated with the aged binder. The Rejuvenating Agent then penetrates the aged binder layer and slowly softens the old asphalt binder. After some time, all the Rejuvenating Agent has penetrated the aged binder and viscosities of both inner and outer layers gradually decrease. Finally, with time, the diffusion process continues until equilibrium is reached.

One of the main factors that must be considered when employing Rejuvenating Agents is the homogeneity of the final binder. For example, suppose the Rejuvenating Agent is not evenly distributed in the recycled mixture. In that case, the mixture will perform differently from point to point, resulting in poor high-temperature rutting performance, poor cracking resistance at low temperature, and high moisture susceptibility of recycled asphalt pavement. Homogeneity

depends on the manufacturing parameters (mixing time and temperature), type of production equipment, method of introducing RA, and type of virgin binder or Rejuvenating Agent. Previous studies show that a partial blending of RA and the virgin binder occurs in most cases, contributing to non-uniform properties. Therefore, to explore the appropriateness of the final mix, mixture performance tests need to be performed.

In the production of recycled pavement, the type and dosage of Rejuvenating Agents need to be appropriately determined so that the low-temperature properties of the mixture can be improved. In contrast, the properties at higher temperatures are not adversely affected. Other parameters to consider are the short and long term criteria. In the short term, the Rejuvenating Agent must diffuse rapidly into RA binder and mobilize the aged asphalt, increasing the workability of the mixture. Most of the diffusion should be completed before the traffic is allowed to avoid reducing friction and increase susceptibility to rutting. For the long-term, the rejuvenated binder should provide sufficient adhesion and cohesion between the aggregate particles to prevent moisture damage and raveling. Another issue is related to the ageing of the rejuvenated binder. It was reported that the ageing of the rejuvenated binder is faster than that of the virgin binder. Therefore, the performance of rejuvenated asphalt mixture should be evaluated (Moghaddam & Baaj, 2016).

It is essential to highlight that reactions may change between RA sources. Therefore, a Rejuvenating Agent that had beneficial effects on one RA source does not necessarily have the same effect on RA collected from another source.

2.3 EFFECTIVENESS EVALUATION OF REJUVENATING AGENTS

If RA content is higher than 20%, it is required to determine binder properties because aged binder might affect binder grade and, therefore, mixture performance. To achieve the characterization, different methods are presented in the literature that could be followed, usually based on the study of RA fractions (aggregates and asphalt binder). They are separated using several methods, including ignition or solvent extraction methods. Although using solvents to extract the aged binder may damage the material's natural composition, causing hardening or changing the actual structure, leaving a residual amount of solvent.

Another factor that must be considered when binder and aggregates are studied separately is that the Rejuvenating Agents' real effects are partially overlapped with the effects due to the mix, such as the aggregation of the grains of the lytic skeleton and aggregate interlocking.

The main disadvantage for both methods is that they cannot determine the precise differences deriving from different Rejuvenating Agents, which can diffuse differently inside the mixture through the oxidized binder film, influencing the rheological characteristics of the type of established bond.

One of the investigations developed about the characterization of the Rejuvenating Agents' effects in RA is the "Influence of six rejuvenators on the performance properties of Reclaimed Asphalt Pavement (RAP) binder and 100% recycled asphalt mixtures" (Martins Zaumanis, 2014). The Rejuvenating Agents employed were Waste vegetable oil, Waste vegetable grease, Organic oil hydrogen, Distilled tall oil, Aromatic extract, and Waste engine oil. Each Rejuvenating Agent was dosed at 12% binder mass for the extracted RA binder and 100% RA mixture. Thus, Rejuvenating Agent dosage was a result of previous investigations.

In the study, the extracted RA binder was tested for PG after adding each of the Rejuvenating Agents to determine the range the reclaimed binder meets Superpave PG 64-22 requirements. The maximum dose was defined to ensure rut resistance (satisfy high PG temperature), while the minimum dose was set by either low PG temperature or intermediate temperature parameter.

During the study were tested three different sample types were:

1. 100% RA and 12% of a Rejuvenating Agent concerning the binder content,
2. "Virgin Mix" sample, composed by 9.5 mm aggregates extracted by removing the binder in an ignition oven blended with 5.94% of virgin PG 64-22 bitumen, which is equal dose to that of the rejuvenated samples (binder + Rejuvenating Agent),
3. "RAP Mix", the virgin binder was added to RA in the proportion of 12%, to evaluate the benefit of simply increasing binder dose rather than adding Rejuvenating Agents,

Figure 3 presents all the tests realized in the Zaumanis investigation; they include rheological type on aged and rejuvenated binder extracted from RA and tests performed on 100% RA and 12% Rejuvenating Agent.

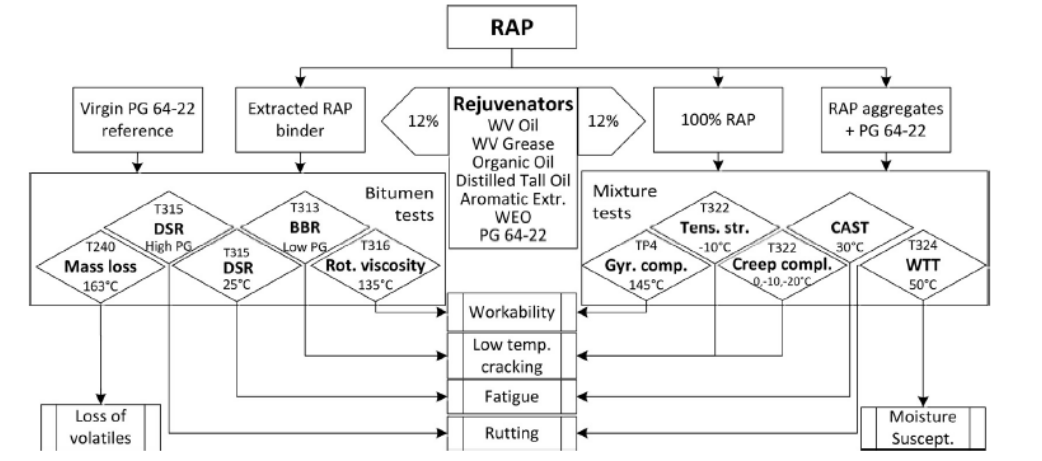

Figure 3. Research plan and test methods for "Influence of six rejuvenators on the performance properties of Reclaimed Asphalt Pavement (RAP) binder and 100% recycled asphalt mixtures" (Martins Zaumanis, 2014).

Finally, some of the conclusions obtained from the "Influence of six rejuvenators on the performance properties of Reclaimed Asphalt Pavement (RAP) binder and 100% recycled asphalt mixtures" (Martins Zaumanis, 2014) were the following:

- Five of the six tested Rejuvenating Agents at 12% dose ensured correspondence to the required PG 64-22 temperature.
- Organic additives proved to be more efficient at reducing PG temperature than petroleum products.
- The high PG for all rejuvenated samples remained above the virgin binder, indicating increased rutting resistance.
- Low-temperature mixture cracking test results showed that five of the six Rejuvenating Agents had decreased cracking susceptibility compared to RA mixture.
- Fatigue resistance of recycled mixtures at the used test parameters was higher than that of virgin mixture for all except for one Rejuvenating Agent.
- The use of all Rejuvenating Agents increased the workability of RA mixture, but none could improve it to the virgin binder or mixture level.

2.4 MODEL SYSTEM FRAMEWORK

In the literature, two alternative approaches can be followed to investigate the effectiveness of the Rejuvenating Agents, one based on the chemical and rheological analysis of extracted binder from RA, adequately mixed with Rejuvenating Agents. However, as explained, this procedure requires using solvents that can damage the extracted binder. The second approach proposed in the literature is the study of bituminous mixtures containing the rejuvenated RA. Nevertheless, this procedure is time and money consuming and superpose the mix dependent

effects with the Rejuvenating Agent results. Therefore, a new approach called the Model System (MS) was developed in the Road Materials Laboratory of Politecnico di Torino.

In " Testing of reclaimed asphalt model systems for the evaluation of the effectiveness of rejuvenators" (Dalmazzo, Urbano, Riviera, & Santagata, Testing of reclaimed asphalt model systems for the evaluation of the effectiveness of rejuvenators, 2020) are presented the results of a preliminary study based on the mechanical testing of MS constituted by a single-sized RA material, in its original state and after pretreatment with Rejuvenating Agents.

The Model System is constituted by a single-sized 5/8 RA material, selected to limit the presence of the finer fractions and RA cluster, ensuring the same granular composition for each MS. MS was designed to obtain a constant value of the Voids in the Mineral Aggregate (VMA) to have a constant lithic structure and similar contact points between aggregates. Therefore, the mechanical behaviour of MS depends mainly on the binder phase, limiting the effect of aggregates interlocking.

The investigation employed a single-sized 5/8 RA, two Rejuvenating Agents (A= Paraffinic hydrocarbon oils, B=non-toxic additives with a vegetal oil base), and a neat virgin bitumen (50/70 penetration grade).

All MS had a VMA target equal to 30%. Using a single sized material with high VMA, the structure will respond under indirect tensile stress that is mainly dependent upon bonding of the binder phase, ultimately affected by employed Rejuvenating Agents, with limited effects due to the aggregate interlocking. The absence of agglomerations and fines in RA material also eliminates other phenomena that may occur during heating and compaction (Dalmazzo, Urbano, Riviera, & Santagata, Testing of reclaimed asphalt model systems for the evaluation of the effectiveness of rejuvenators, 2020). It is essential to underline that model systems do

not reproduce bituminous mixtures constituted by 100% RA conceived with a continuous grading and exhibit a response under loading similar to standard asphalt mixtures.

In the investigation, three different MS were studied:

- The black system (BS) constituted by 100% RA
- Rejuvenated systems (RS) composed of RA+A or RA+B
- The white system (WS) that is the reference system, made of aggregates from RA with virgin bitumen, with a dosage equal to that of RA

The following picture presents the standard structure to all model systems on the left side with constant and controlled volumes of solid aggregate skeleton and binder. Moreover, the phase distribution for each system is shown on the right side.

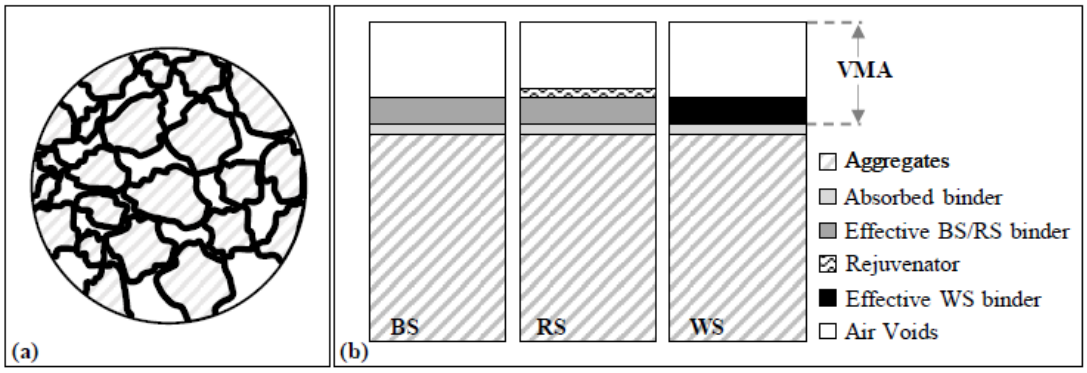

Figure 4. Model systems evaluated in "Testing of reclaimed asphalt model systems for the evaluation of the effectiveness of rejuvenators" (Dalmazzo, Urbano, Riviera, & Santagata, Testing of reclaimed asphalt model systems for the evaluation of the effectiveness of rejuvenators, 2020)

After the compaction, the tests developed during the study were stiffness modulus ITSM and indirect tensile strength ITS as a function of curing time.

As an experimental result, the curing time did not affect the mechanical behaviour of the Model systems. The quantification of the rejuvenating effects is also realized by analyzing the

behaviour for stiffness, strength, and ductility toughness index. In general, the presence of the Rejuvenating Agents restored the stiffness properties of RA binder and increased the compressive strain al failure. The tests realized also allowed the comparison among the two Rejuvenating Agents employed.

In conclusion, the investigation realized by Dalmazzo, Urbano, Riviera, and Santagata, using the Model systems, shows that the proposed approach is auspicious, allowing the assessment of their response under loading with no alteration of their structure and composition.

3. MATERIALS PROPERTIES AND COMPOSITION

First, it is essential to recognize the required materials to develop the present thesis, the composition, properties, and characteristics of Reclaimed Asphalt, Rejuvenating Agent and Virgin binder employed. Knowing the materials and the differences between the diverse origins will be clearer to understand the mechanical behaviour and the results obtained in the tests realized. The source, characteristics, and laboratory procedures to obtain the respective properties are presented for each material.

3.1 RECLAIMED ASPHALT (RA)

As previously exposed, the Reclaimed Asphalt Pavement is an aged material that has already lost its original properties and is obtained from removing and crushing damaged asphalt pavements.

The material used came from three different asphalt plants close to Turin metropolitan area; therefore, three sources named B, C and S were employed. Each RA is a mix of materials milled from asphalt pavements and have various ages, lithological components, gradation, and bitumen types, among others. Of course, for such reasons, the three RA are different between them.

Figure 5. The feedstock of RA source B

From the sources, two RA types were taken, the feedstock that allowed the knowledge of the real structure of the whole material and the 5/8 that was employed in the definition of Model System.

The feedstock characteristics depend on the type of processes that RA underwent in the plant, related to the fractioning of RA. Therefore, based on the sieve size distribution analysis, RA from the feedstock can be classified according to the nomenclature established in EN 13108-8.

Both RA from stockpile and 5/8 were dried at ambient temperature and, also 5/8 RA was cleaned to ensure that it did not contain material smaller than 5 mm or greater than 8 mm.

Figure 6. Drying material process

Then the sample reduction was realized following the normative EN 932-2 to obtain a homogeneous representative sample.

Figure 7. Riffle box employed to realize sample reduction

3.1.1 SIEVE DISTRIBUTION

The particle size distribution determination was obtained following the EN 12697-2. The sieve analysis was carried out for RA and its extracted aggregates to obtain the black and white gradation curve, respectively.

The sample preparation followed the standard EN 12697-39. First, the automatic sieving machine realized the sieving and then was repeated manually to verify it. First, the material was directly poured into the sieving column organized from top to bottom in decreasing order of aperture. The material mass retained by each sieve was registered. The test was realized two times per material type. Then, the passing average was computed to plot the respective granulometric curve.

Figure 8. Automatic sieving machine

Figures 9 and 10 show the black curve for feedstock and 5/8 RA for each source.

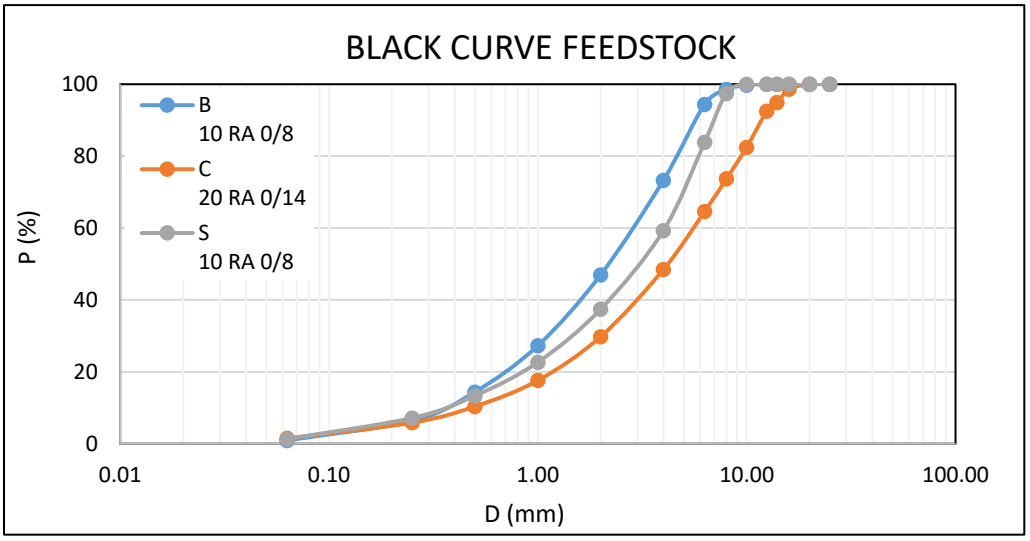

Figure 9. Black curve for Feedstock material

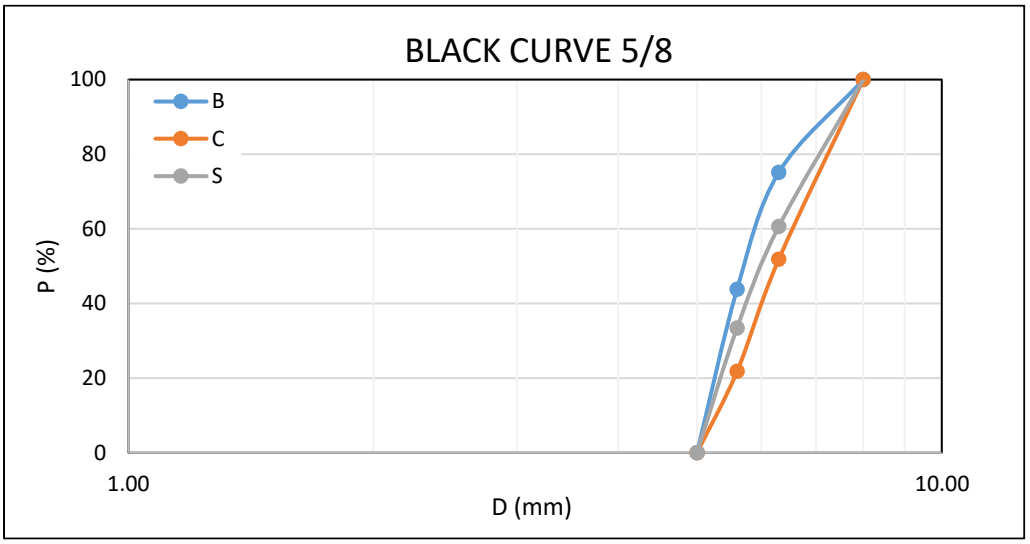

Figure 10. Black curve for 5/8 material

To compute the white gradation curve, first was necessary to eliminate the binder content by ignition. Then, wash the material to eliminate the filler (<0.063 mm), avoiding losing the fine part; the weight of the filler was computed as the difference of the weights before and after the washing procedure, the standard followed is the EN 933-1. After, the retained material in the 0.063 sieve was dried at 110± 5 ºC until the constant mass was reached, and the same sieving procedure explained for the black curve was repeated with the white material.

Figures 11 and 12 show the results for the white curve for feedstock and 5/8 RA for each source.

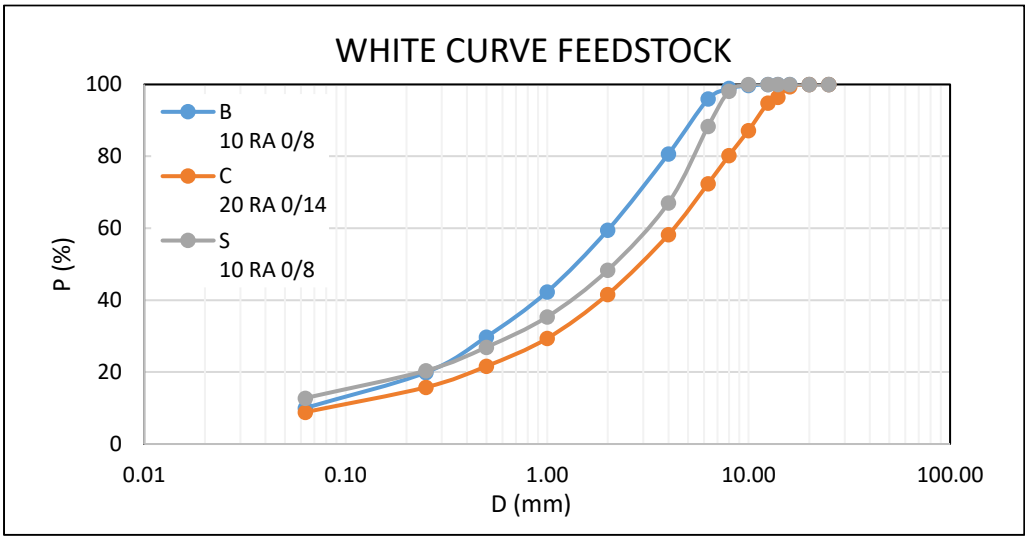

Figure 11. White curve for Feedstock material

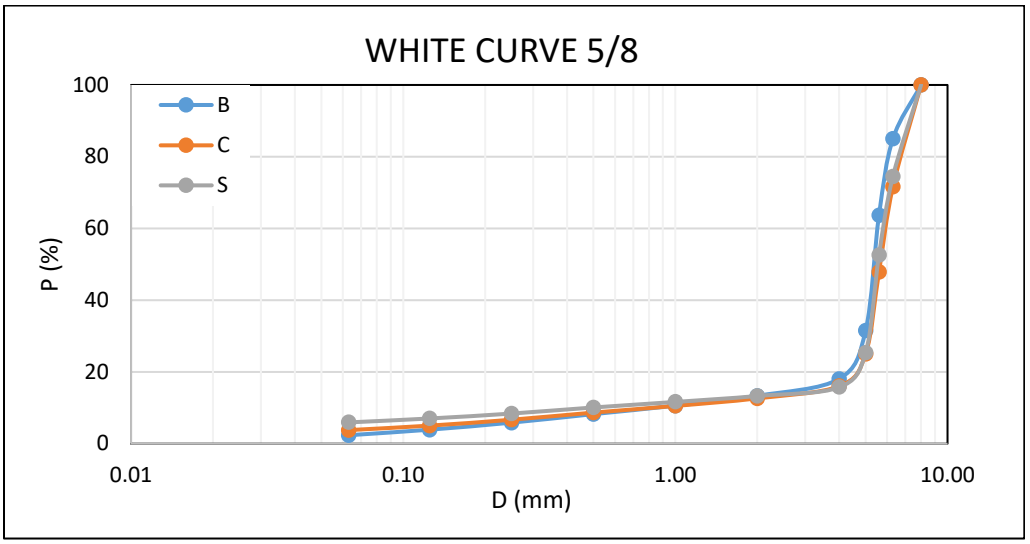

Figure 12. White curve for 5/8 material

3.1.2 BINDER CONTENT BY IGNITION

According to the ignition method, the binder content was determined following the EN 12697-39. The material was prepared according to EN 12697-28. It was spread homogeneously into a sample chamber and then placed into a furnace at 540 ºC.

Figure 13. Sample chamber with spread material and Carbolite.

Then, the difference of the sample weight before and after the ignition procedure provided the binder in RA weight. After the binder percentage was computed, it can be calculated concerning the weight of RA (%B RA) and aggregates (%B AGG).

$$\%B\ RA = \frac{Wmixture - Waggregate}{Wmixture} \cdot 100$$

$$\%B\ AGG = \frac{Wmixture - Waggregate}{Waggregate} \cdot 100$$

The procedure was realized at least two times per RA source, and the results for the feedstock and 5/8 are presented in Table 1.

Table 1. Binder content for feedstock and 5/8 material

	%B RA Average (%)	%B agg Average (%)
B 5/8	3.5	3.6
C 5/8	3.1	3.2
S 5/8	2.8	2.8
B 10 RA 0/8	5.8	6.1
C 20 RA 0/14	4.4	4.6
S 10 RA 0/8	5.0	5.3

3.1.3 DETERMINATION OF MAXIMUM DENSITY

The determination of the maximum density (voidless mass) followed the EN 12697-5 by the volumetric procedure for each source, for black, white, and rejuvenated system. The samples of the bituminous mixtures were obtained following the EN 12697-27.

First, the weight and volume of the pycnometer and the correspondent headpiece must be known. Then, the prepared sample was placed and registered the weight. Next, the pycnometer was filled with filtered water, and the entrapped air was evacuated applying a partial vacuum for about 30 minutes. Later, the pycnometer and the headpiece were filled with de-aired water creating a meniscus at the top of the lid, and the weight and temperature were registered. Thus, for each material type, the procedure was realized two times.

Figure 14. Computation of Maximum density

Then the Maximum density was computed as:

$$\rho_{mv} = \frac{m_2 - m_1}{10^6 V_p - (m_3 - m_2)/\rho_w}$$

where,

ρ_{mv} is the maximum density of the bituminous mixture computed by the volumetric procedure (kg/m^3)

m_1 correspond to the mass of the pycnometer plus the headpiece (g)

m_2 mass of the pycnometer plus the headpiece and the sample (g)

m_3 mass of the pycnometer plus the headpiece test sample and de-aired water (g)

V_p the volume of the pycnometer filled up to the top creating a meniscus (m^3)

ρ_w the density of the water according to the temperature (kg/m^3)

Table 2. Maximum Density results

		TMD
		kg/m³
B	10 RA 0/8	2526
	5/8 RA	2628
	5/8 White	2579
	5/8 + E8%	2620
	5/8 + P8%	2622
C	20 RA 0/14	2614
	5/8	2669
	5/8 White	2624
	5/8 + E10.5%	2631
	5/8 + P14.5%	2642
S	10 RA 0/8	2555
	5/8	2664
	5/8 White	2626
	5/8 + E8%	2647
	5/8 + P8%	2648

3.1.4 DETERMINATION OF PARTICLE DENSITY AND WATER ABSORPTION

As it is established in the standard EN 1097-6, the apparent particle density is the ratio between the oven-dried mass of an aggregate sample and the volume that it occupies in water, including the volume of any internal sealed voids but excluding the volume of water in any water accessible voids.

First, the aggregates must be extracted from RA, then divide the sample into different subsamples according to their size, greater than 4 mm and smaller than 4 mm but greater than 0.063 mm. Then, it was required to report the weight of the sample in the saturated and surface-dried condition and again in the oven-dried condition, and the volume of it considering the mass of the water displaced by the pycnometer method. The test was done with two repetitions for the feedstock material and 5/8 mm.

3.1.4.1 PARTICLES BETWEEN 0.063 AND 4 MM

The sampling was prepared following EN 932-1. First, the material was washed to remove smaller particles. Next, using a pycnometer, the material was immersed in water for 24 hours; then, the entrapped air was removed using a vacuum for 30 minutes. After, the pycnometer was overfilled by adding de-aired water until the meniscus was created on top of the cover. Finally, the weight and temperature were registered.

Figure 15. Pycnometers with samples immersed vacuum process

Next, most of the water of the pycnometer was decanted, and the remaining part was placed into a tray. The material placed on the tray must be exposed to a current of warm air to evaporate the surface moisture; it was stirred constantly, ensuring that the drying was uniform. To know

if the surface dried state was achieved, a test with a metal cone was realized: the cone was placed with the largest diameter facing the tray downwards, then it was filled with the material and using a metal tamper was tamped 25 times, letting it fall by its weight. After, the cone was lifted. If the aggregate did not collapse, it meant that it was still too wet, the drying was continued. The cone test was repeated until the collapse situation happened at the mould removal, being careful to not over-dry the material. Then it was weighed and dried in the oven at 110ºC until it reached constant mass, let cool, and weighted again.

The following picture presents the different stages that material must pass before achieving saturated and surface dried conditions. The first one is clear how the aggregates maintained the shape of the cone. In the second picture, the structure is not more maintained but still does not present the characteristic shape shown in the last picture.

Figure 16.Procedure to obtain saturated dried surface condition

Finally, the particle densities and water absorption were computed:

$$\rho_a = \rho_w \frac{M_4}{M_4 - (M_2 - M_3)}$$

$$\rho_{rd} = \rho_w \frac{M_4}{M_1 - (M_2 - M_3)}$$

$$\rho_{ssd} = \rho_w \frac{M_1}{M_1 - (M_2 - M_3)}$$

$$WA_{24} = \frac{100(M_1 - M_4)}{M_4}$$

where,

ρ_a is the apparent particle density

ρ_{rd} is the oven-dried particle density

ρ_{ssd} is the saturated-surface dried particle density

WA_{24} is the water absorption after immersion for 24 hours

ρ_w is the density of water at the respective temperature

M_1 is the mass of the saturated and surface-dried aggregate in air

M_2 is the mass of the pycnometer containing the sample of saturated aggregate and water

M_3 is the mass of the pycnometer just filled with water

M_4 is the mass of the oven-dried test portion in the air

Table 3 are reported the results of the test

Table 3. Particle density and water absorption results for particles between 0.063 and 4 mm

		Average			
		ρa	**ρrd**	**ρssd**	**WA24**
		(kg/m³)	**(kg/m³)**	**(kg/m³)**	**(%)**
B	**5/8**	2796	2770	2779	0.332
	10 RA 0/8	2762	2759	2760	0.041
C	**5/8**	2780	2774	2776	0.081
	20 RA 0/14	2824	2769	2789	0.693
S	**5/8**	2796	2794	2794	0.028
	10 RA 0/8	2782	2754	2764	0.374

3.1.4.2 PARTICLES GREATER THAN 4 MM

The densities for the particles greater than 4 mm were realized following the normative EN 1097-6, using the pycnometer method. This normative provides the minimum mass of the test portion. After preparing the test portion, it was immersed in water for 24 hours in the pycnometer; then, the entrapped air was removed using the vacuum. Next, the pycnometer was overfilled until the meniscus on top of the cover was created. At this point was registered weight and temperature. Next, the aggregate was removed, letting it drain for some minutes, then it was transferred onto a dry cloth. When the cloth was full of water and could not remove more moisture, the sample was placed in a second dry cloth spreading it and letting it dry at ambient temperature until the aggregate had no more water on the surface, but the appearance was still damp.

Figure 17. Sample (>4 mm) placed onto a dry cloth with saturated and surface-dried condition

The sample was placed in a tray, and the aggregate was weighted. Then it was dried in an oven until it reached constant mass and registered the weight again. Finally, the densities were computed following the same formulas as it was performed for the particles between 0.063 and 4 mm. Table 4 presents the results; the test was realized twice per aggregate type and computed the average.

Table 4. Particle density and water absorption results for particles greater than 4 mm

		Average			
		ρa	**ρrd**	**ρssd**	**WA24**
		(kg/m^3)	**(kg/m^3)**	**(kg/m^3)**	**(%)**
B	**5/8**	2787	2703	2733	1.110
	10 RA 0/8	2780	2704	2732	1.010
C	**5/8**	2839	2768	2793	0.898
	20 RA 0/14	2859	2857	2857	0.024
S	**5/8**	2794	2710	2740	1.107
	10 RA 0/8	2795	2711	2741	1.104

3.2 REJUVENATING AGENT

The Rejuvenating Agents used in the investigation of the present thesis are the E and P. In Table 5 the most important characteristics and properties of the materials are presented; information was taken from the respective datasheet.

Table 5. Properties and characteristics of Rejuvenating Agents

Rejuvenating Agents	**Identification**	**Density**	**Viscosity at 20°C**	**Flashpoint**	**Odour**	**Colour**
E	Plant-based non-toxic additive	0.88 g/cm^3	47 mm^2/s	>220 °C	Odorless	Light yellow
P	A mixture of paraffinic hydrocarbon oils	0.98 g/cm^3	500 cP	>125 °C	Characteristic	Dark yellow

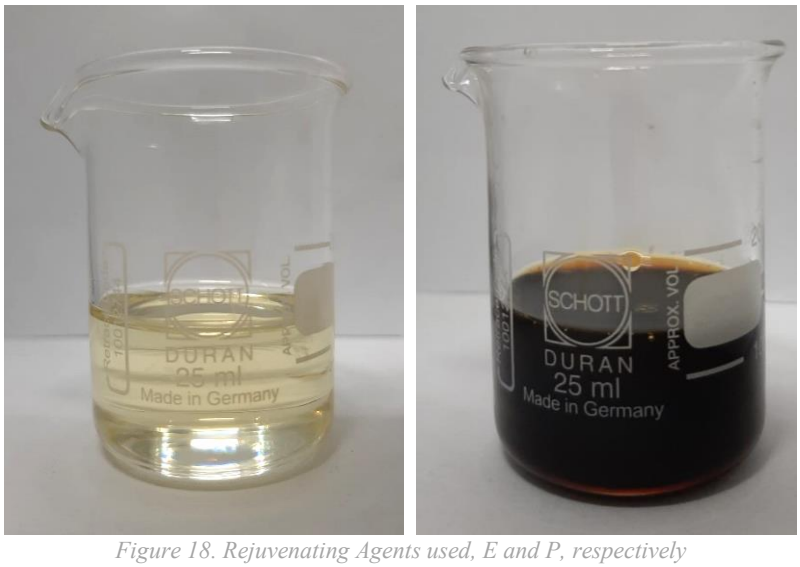

Figure 18. Rejuvenating Agents used, E and P, respectively

3.3 VIRGIN BINDER

During the experimentation, a neat virgin binder with a 50/70 dmm penetration grade was employed to define the reference MS. No tests were developed for the bituminous binder.

Figure 19. Virgin binder employed

4. METHODOLOGY OF TESTING

The poor performance characterizes the mechanical behaviour of RA mixture because of the presence of aged and stiff RA bitumen. A wrong design can increase the possibility of premature pavement distresses, fatigue, and low temperature cracking failures. Therefore, to properly maximize RA recycling is necessary to employ the Rejuvenating Agents and evaluate the effectiveness of such additives in restoring the chemical and rheological properties of RA binder.

After the characterization of the materials used in the present investigation, the thesis objective was pursued: to validate the previous investigations on the Model System (MS) using three different RA sources, combined with two different Rejuvenating Agents, in order to assess the possible dependency of the rejuvenating effects on RA. Therefore, it was required to perform the Dynamic modulus test, which allowed the study of the viscoelastic response, and the definition of the optimum dosage, the Indirect tensile stiffness modulus test (ITSM), and Indirect tensile strength test (ITS) that permitted to evaluate the mechanical performance when Rejuvenating Agents were employed. In order to realize those tests, several samples were prepared through the gyratory compactor, which compaction results allowed the study of the workability for all the study cases.

The Model System is constituted by a single-sized 5/8 RA material, selected to limit the presence of the finer fractions and RA cluster, ensuring the same granular composition. In addition, MS was designed to obtain an equal value (30%) of the Voids in the Mineral Aggregate (VMA) to have a constant lithic structure and similar contact points between aggregates. Therefore, using a single sized material with high VMA, is the mechanical

behaviour will be mainly dependent upon bonding of the binder phase, ultimately affected by employed Rejuvenating Agents, with limited effects due to the aggregate interlocking. The absence of agglomerations and fines in RA material also eliminates other phenomena that may occur during heating and compaction (Dalmazzo, Urbano, Riviera, & Santagata, Testing of reclaimed asphalt model systems for the evaluation of the effectiveness of rejuvenators, 2020).

4.1 SAMPLES PREPARATION

Once the characteristics of MS and the properties of the materials that constitute MS (density, binder content and particles size distribution) have been defined, several samples were prepared employing the gyratory compactor. Three types of MS were considered:

- A black system (BS) made with 100% 5/8 RA;
- A rejuvenated system (RS) composed of 100% 5/8 RA mixed with the Rejuvenating Agent (E or P);
- A white system (WS) constituted by the aggregates extracted from RA mixed with 50/70 neat binder, keeping constant the percentage of the binder characteristic of each 5/8 RA source.

Based on the type of test that will be performed, the samples were compacted in order to achieve a final thickness of 130 mm or 65 mm. The mass of 5/8 RA was defined to have compacted samples with a target of Voids in Mineral Aggregate (VMA) equal to 30%. From the equations presented in the MS-2 Asphalt Mix Design Methods in Chapter 5, “Volumetric Properties of Compacted Paving Mixtures” (Asphalt Institute, 2014), could be obtained the relationship between mass and the Voids in Mineral Aggregates as follows:

$$VMA = 100 - \frac{G_{mb}P_s}{G_{sb}}$$

$$G_{mb} = \frac{M}{V_{geo}}$$

$$M = V_{geo}(100 - VMA)\frac{G_{sb}}{P_s}$$

Where,

M is the mass of the sample

VMA correspond to the voids in mineral aggregate

G_{mb} is the bulk specific gravity of the paving mixture

G_{sb} is the bulk (dry) specific gravity of the aggregate

P_s is the percentage of aggregate by total mix weight

V_{geo} is the geometric volume of the specimens, that will depend on the height (65mm or 130 mm)

The temperature of compaction was 150ºC ± 5°C.

According to the different MS employed, different mixing procedures were followed. First of all, 5/8 RA, the extracted aggregates, the virgin binder and the moulds were placed into the oven at 150ºC; achieved the compaction temperature, 5/8 RA was placed in a preheated mixer.

Concerning BS, 5/8 RA was manually mixed for 5 minutes to obtain a homogeneous material. Then, 5/8 RA was placed inside the hot mould using a funnel and placed again into the oven for 30 minutes to avoid temperature loss during the procedure. Finally, the sample was compacted.

Figure 20. Mixing procedure for RA samples

Instead, the preparation of RS required the mixing of 5/8 RA for one minute. Then, half of the Rejuvenating Agent was added and were mixed for another minute. Finally, the rest of the Rejuvenating Agent was poured, and the sample was mixed for another 3 minutes, mixing in total 5 minutes. Next, the sample was placed using a funnel inside the hot mould, placed into the oven for 30 minutes, and compacted.

Figure 21. Rejuvenating Agent weight

Finally, WS was prepared with the aggregated extracted (using the ignition oven) from 5/8 RA, thereafter heated at the compaction temperature and placed in the preheated mixer along with

the virgin bitumen in equal quantity to that constituted 5/8 RA. Then, all components were mixed for 5 minutes, poured inside the hot mould, and placed into the oven for 30 minutes. Finally, the sample was compacted.

4.1.1 WORKABILITY

Following the normative EN 12697-31, the compaction of the specimens was developed using a gyratory compactor. As a result, specimens of specified height at a predetermined density were prepared, and a density curve can be determined as the degree of compaction versus the number of gyrations.

Figure 22. Gyratory compactor machine employed

The parameters fixed in the machine were: vertical pressure of 600 KPa, the rotational angle of the mould axis 1.25º, and the compaction height target 65 mm or 130 mm. The required mass to obtain the voids volume target, 30%, was computed as established before.

The compaction is realized by reorganizing the aggregates thanks to applying a static compression and shear action that changes the direction constantly because of the eccentric rotation of the mould; this action simulates the real forces applied in the construction site. Figure 23 represents the forces applied in the gyratory compactor machine.

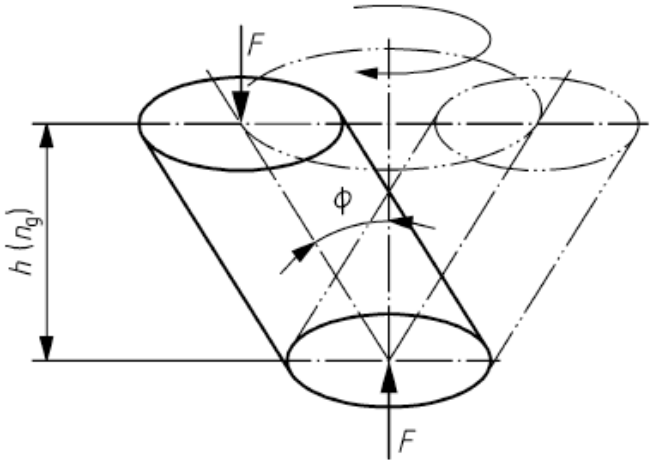

Figure 23. Gyratory compactor principle, picture taken from EN12697-31

When the mass and the other fixed parameters have been defined, the compaction of the specimens was developed. The gyratory machine, during the procedure, recorded the variation of specimen height as a function of rotations.

Figure 24. Specimens after compaction procedure

As the geometric volume, maximum density and the effective mass of the sample were known, it was possible to construct the compaction curve and obtain the following essential parameters:

- C is the degree of compaction
- C1 is the self-compaction, the value of the degree of compaction for the first gyro.

- k workability represents the compaction gradient, how easy it is to mould a specimen.

These parameters describe the behaviour of the material as:

$$C_{(nG)} = C_1 + k \cdot \log(n_G)$$

As an example, the compaction curve for a RA specimen of B source is reported. In the y-axis is presented the compaction degree, and in the x-axis is shown the logarithm of the number of gyrations. It also indicates the equation of the line and the coefficient of determination. For this case, the value of k is 8.088, and the value of C_1 corresponds to 59.482.

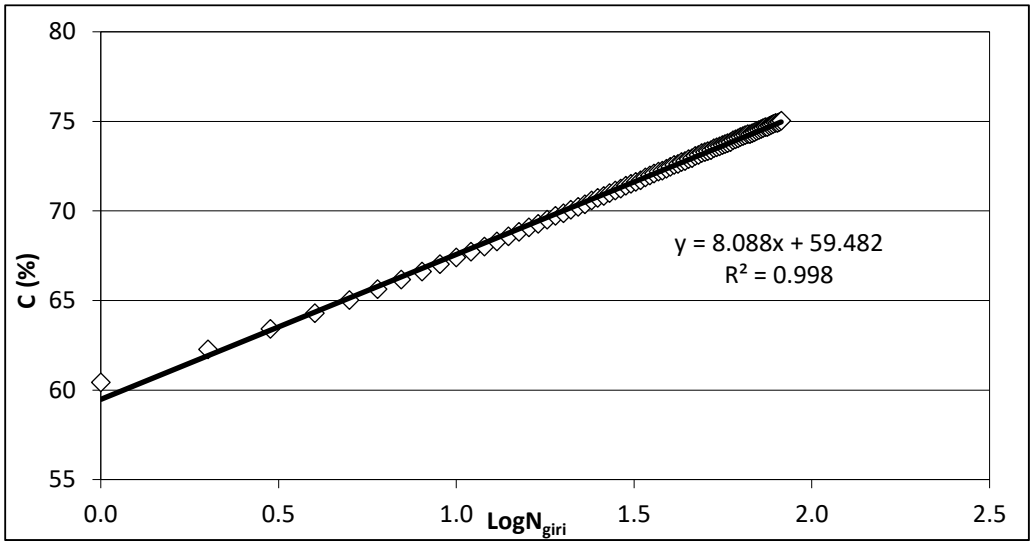

Figure 25. Compaction curve for RA B source

In order to realize the tests specified previously, specimens of 100 mm diameter and 65 mm or 130 mm height were compacted for each MS and RA source. It is clear that even if the material properties and the geometry of samples change, all samples will maintain similar volumetric properties imposed by MS. Therefore, for ITSM and ITS, samples of 65 mm height were used, while the ones of 130 mm were employed for the dynamic modulus test and cyclic direct tension test.

Figure 26. Specimens of 65 mm and 130 mm for C source

The nomenclature used to recognize the different samples is the following:

XY-ab-c

Where

- X, R=RA or B=White system
- Y, RA or aggregates source B, C, or S
- a, Rejuvenating Agent source (E, P, 0 = black or white system)
- b, Rejuvenating Agent dosage (0 = black or white system)
- c, sample ID

4.2 DYNAMIC MODULUS TEST

RA is a viscoelastic material because of the properties provided by the bitumen included in the material. Therefore, it was decided to validate the previous investigation in the linear viscoelastic field, maintaining the linear relationship between stress and strain and the response as a function of the temperature and frequency.

The dynamic modulus test was carried out following the standard AASHTO T378-17. Each specimen was subjected to a controlled sinusoidal compressive stress of various frequencies at a defined temperature without confining pressure. As established in the standard, the applied stresses and resulting axial strains were measured as a function of time and were used to measure the dynamic modulus and phase angle.

After the compaction of the samples, the gauge points were attached to the specimen spaced 120º from each other. Then, the samples were conditioned in a chamber, for the tests realized at 4ºC, and 20ºC specimens were conditioned overnight. Instead, for the tests performed at 40ºC, samples were conditioned four hours. After the specified time, the test was accomplished in the 30 kN servo-hydraulic Universal Testing Machine (UTM-30).

Figure 27. UTM-30 machine

As the standard AASHTO T378-17 established, it was required the use of platens and friction reducers and the system must be assembled from bottom to top as: bottom loading platen, bottom friction reducer, specimen, top friction reducer, and top loading platen.

Figure 28. Configuration of Dynamic modulus test in UTM-30

Then, three LVDTs were installed on the gauge points. Finally, the test was started when the temperature was established at the target value.

The parameters defined for each test were:

- The frequencies at which the test was performed: 25 Hz; 20 Hz; 10 Hz; 5 Hz; 2 Hz; 1 Hz; 0,5 Hz; 0,2 Hz; and 0,1 Hz
- Target test temperature: 4ºC, 20ºC and 40ºC
- Axial gauge length: 70 mm
- Conditioning time: overnight or 4 hours, depending on temperature
- Average dynamic strain range from 75 to 125 micro-strain
- Contact stress equal to 5%
- Dimensions of the sample

For each imposed load, ten conditioning cycles were realized to obtain the force that had to be applied to generate a deformation level within the target range. Then ten loading cycles were applied to compute the Dynamic modulus and phase angle.

At the end of the procedure, the software provides the dynamic modulus and the phase angle. Therefore, the computation of the black diagrams and the master curves was possible. The black diagram was used to check the quality of the test data without considering the effect of frequency and temperature; if the results were of good quality, the shape of the curve was smooth and continuous. Figures 29 and 30 present two examples of black diagrams, one for BS and the other for WS.

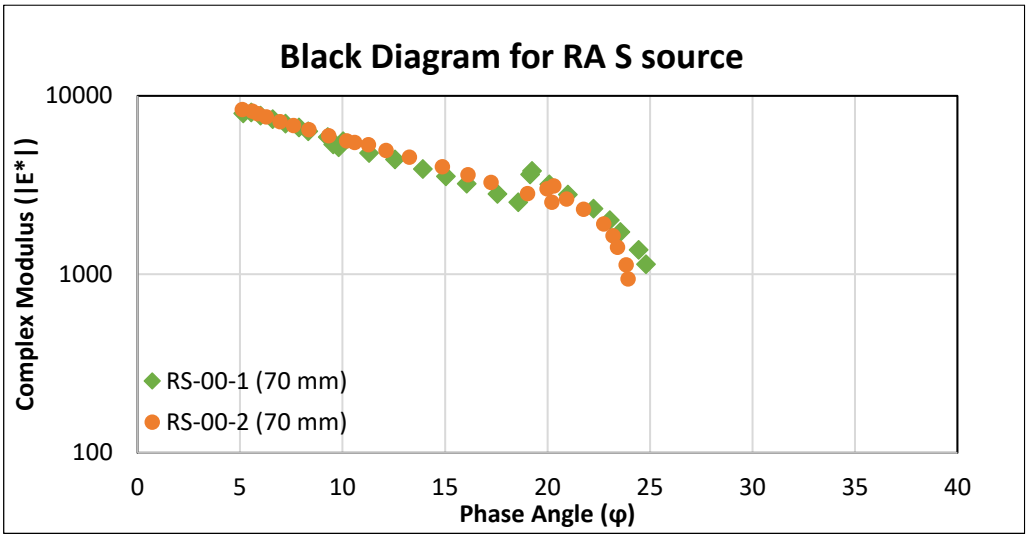

Figure 29. Black diagram for BS S source

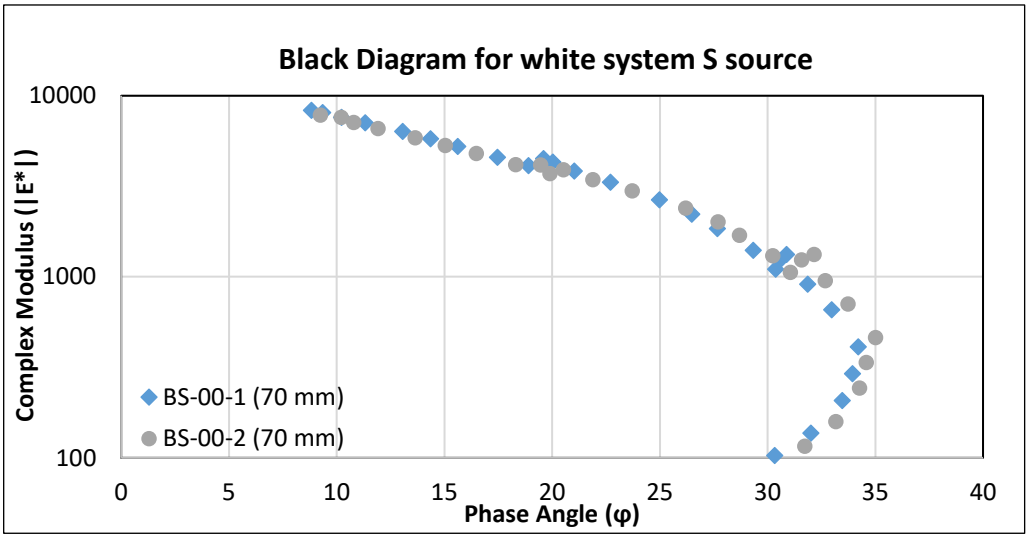

Figure 30. Black diagram for White system S source

The difference between the graph shape for both systems at high temperatures is notorious, where the specimen behaviour mainly depends on the solid skeleton composition. For BS, a stiff binder that covered the aggregates without allowing them to get in contact was studied, showing the aged bitumen's performance. While for WS case composed by a virgin binder, at high temperatures, the binder flowed and aggregates started to get more in contact, where its response can be appreciated changing the trend of the graph into a C shape.

Raw data were post-processed to construct the dynamic modulus and phase angle master curves that represent the mechanical behaviour of the material at different temperatures and frequencies (Kim, 2009). In addition, the sigmoidal function was also fitted to the raw data to analyze the linear viscoelastic behaviour of each MS. The following formula evaluates the sigmoidal fitting function:

$$\log(|E^*|) = \delta + \frac{\alpha}{1 + e^{\beta - \gamma \log(\xi)}}$$

Where,

$|E^*|$ dynamic modulus

δ minimum modulus value

α span of modulus values

β, γ shape parameters

ξ reduced frequency

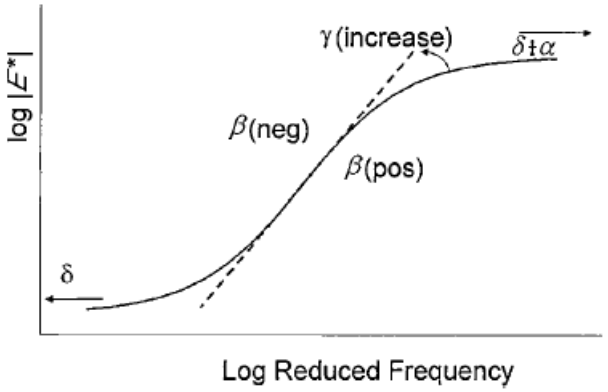

Figure 31. Sigmoidal function. (Kim, 2009)

The master curves are limited between two horizontal asymptotes: the upper, defined at low temperatures as a function of the binder limiting stiffness, and the lower, at warm temperatures, mainly influenced by the solid skeleton composition. While the master curves are a powerful tool to estimate the viscoelastic properties of each MS, it was also used to define the optimum dosage of each Rejuvenating Agent.

The optimum dosage of a Rejuvenating Agent is defined as the percentage to be added to RA so that the linear viscoelastic response of RS is comparable with the reference one, for this case, WS. Graphically it is evidenced when the master curve of RS overlaps with that of WS.

Nevertheless, the overlapping is mainly achieved at low and medium temperatures and rarely at high temperatures. This behaviour is because the Rejuvenating Agent does not totally blend in the aged binder, and some of the rejuvenated RA remain as black rocks. At high temperatures, the dynamic modulus is mainly influenced by the solid skeleton and makes visible the behaviour, hindering the overlapping of the virgin and rejuvenated master curves.

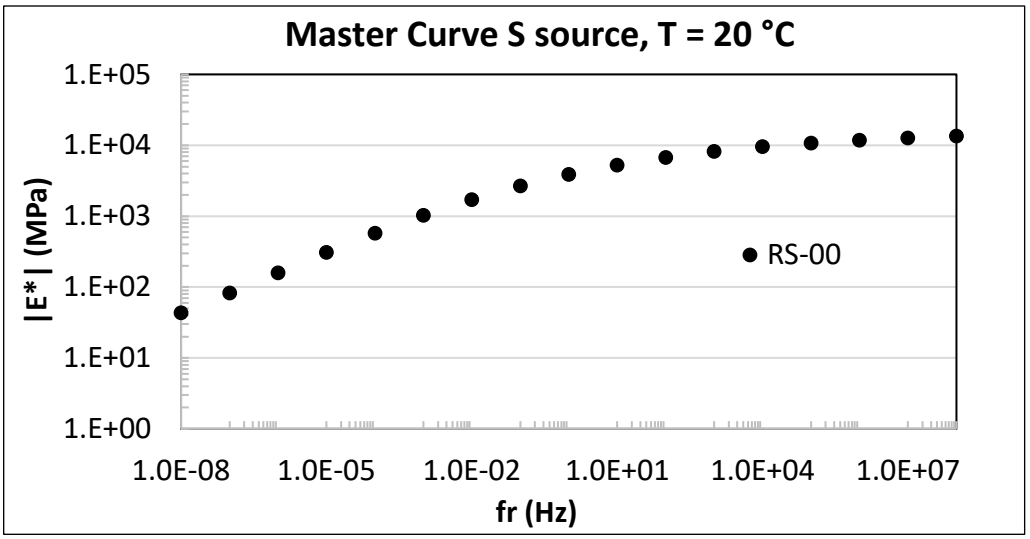

Figure 32. Master curve example for RA S source

As it was established, the gauge length used was 70 mm, as the standard suggests. However, the development of the test was also studied using different gauge lengths in samples of 130 mm and 65 mm height. Accordingly, for samples of 130 mm height, four different gauge lengths were considered:25 mm, 35 mm, 70 mm, and100 mm. In addition, two gauge lengths were adopted for 65 mm thick samples; 25 mm and 35 mm. The choice to perform the test with different gauge lengths and sample thickness was an attempt to understand how the gauge length itself influences the measure and if the dynamic moduli measured on 130 mm samples were similar (for a particular gauge length) to those measured on 65 mm samples. The dynamic modulus test performed on 65 mm samples can be considered unconventional because the AASHTO standard requires samples with a thickness of 130 mm. However, if results are reliable and comparable to those obtained with the standard geometry, fewer efforts and less 5/8 RA quantity could be employed to analyze the linear viscoelastic properties of each MS.

Figure 33. Samples of 130 mm and 65 mm with different gauge points

After the analysis of test results was evident that the complex modulus |E*| presents a variation concerning the gauge length, the modulus increases as GL decreases. In Figures 34 and 35, the behaviour is shown.

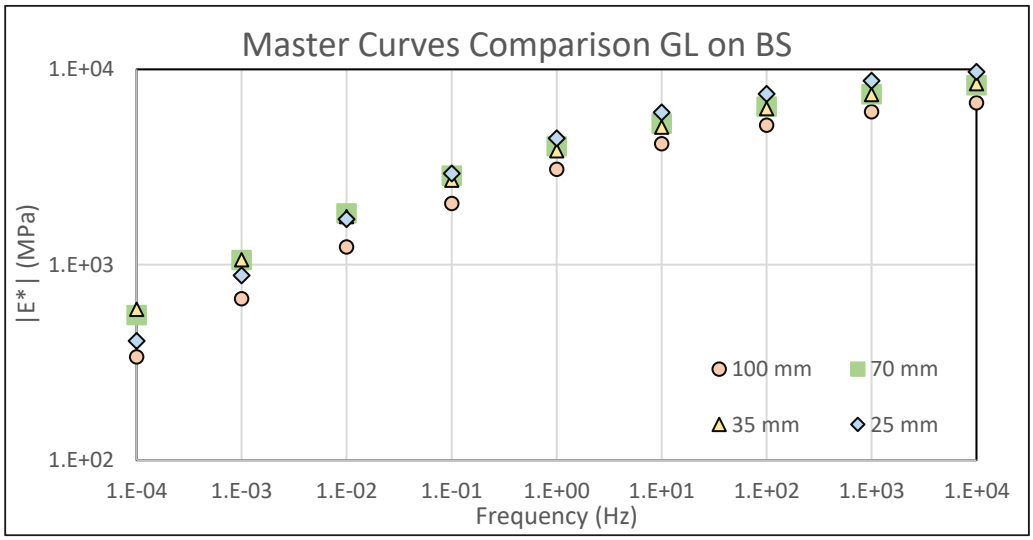

Figure 34. Master curves comparison for different gauge lengths on 130 mm samples

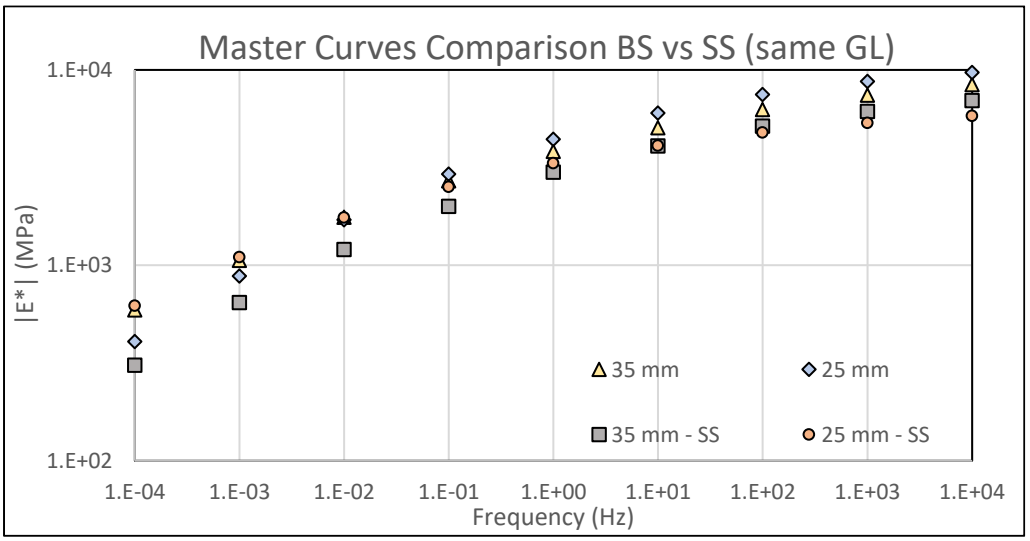

Figure 35. Master curves comparison for 130 mm and 65 mm samples at 35 and 25 mm GL

This result can be justified by considering the degree of compaction that changes within the sample. Moving from the top or the bottom toward the middle of the specimen, the compaction level increases, meaning less air voids, and therefore an increase of the stiffness is obtained.

Also, during the test, signal noises were noticeable on 130 mm samples with a gauge length of 35 mm and 25 mm and in all measurements with small samples. In conclusion, the only good measurements were reached at 100 mm and 70 mm. Therefore, it was decided to follow the standard and maintain the gauge length for all tests equal to 70 mm.

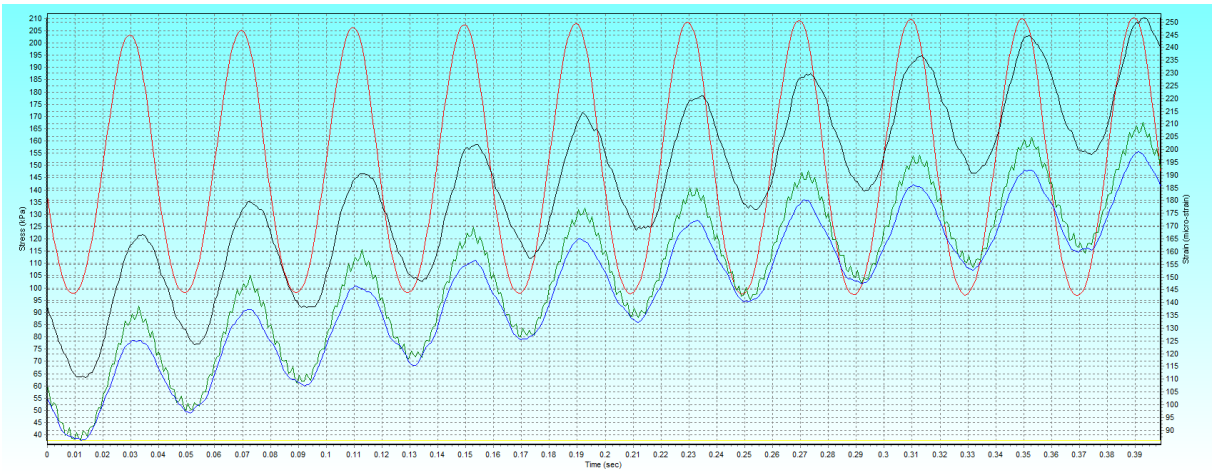

Figure 36. Signal noise in the test for RB-00-2 at 35 mm, 40ºC, 25 Hz

4.3 INDIRECT TENSILE STIFFNESS MODULUS (ITSM) TEST

The elastic modulus measured by the indirect tensile test was computed following EN 12697-26C.

For this non-destructive test, the specimens with 100 mm diameter and 65 mm height were used. The required test equipment includes the UTM-30 machine, steel loading frame, LVDT mounting frame and two linear variable displacement transducers (LVDTs).

Figure 37. LVDT mounting frame and example of test equipment.

This test was included in the experimental program to study if its results for the black and white model systems were correlated to the dynamic modulus test outcomings, using the same materials but different geometry. One of the goals of studying this relationship was to permit the characterization of the stiffness by alternative tests, allowing the classification of performance of pavements using a smaller sample that requires half of the material compared to the sample used for the dynamic modulus test. This advantage reduces the costs of materials and sample preparation time; it is also a more straightforward test to develop for the operator.

As established in EN 12697-26, the specimen is deformed in its linear range under controlled strain. Then using the measured force and deformation signal reported by the LVDT, the stiffness modulus can be computed:

$$E = \frac{F}{\Delta * h} * (0.273 + v)$$

Where:

E is the elastic stiffness modulus (MPa)

F is the loading force (N)

Δ is the amplitude of the resilient horizontal deformation obtained during the load cycle (mm)

h is the thickness of the specimen (mm)

v is the Poisson's ratio

The sample was subjected to a vertical load through the machine actuator, which distributed the load thru the two stainless steel loading strips that were in contact with the specimen by a concave surface. Therefore, the load actuator could apply repeated load pulses with a rest period.

The deformations generated by the loading effect were read by a pair of LVDT's on the horizontal diameter of the sample. It implied that despite the type of load being compression, the deformations were distributed along the vertical plane, therefore, of tension.

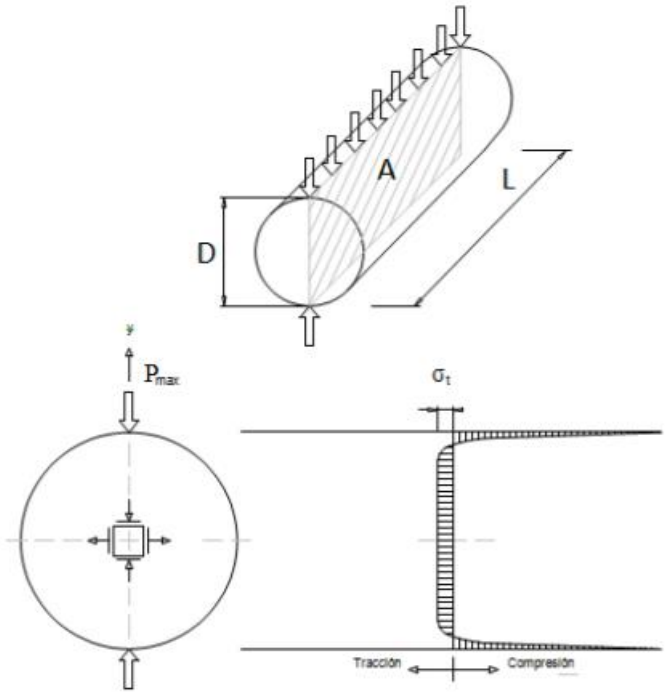

Figure 38. Stress state of the sample during the test. (VARGAS & NEUMANN, 2016)

The main test parameters were the target horizontal deformation (5 με), temperature (20ºC), loading time (50, 100, 125, 150, and 200 ms), conditioning pulses (10), and specimen dimensions.

Before the test, samples were conditioned overnight at the specified temperature. Then, the specimen was mounted to the frame, ensuring that the clamping was even without over-tightening them.

The stiffness modulus was evaluated along two different diameters perpendicular to each other.

The machine applied ten conditioning pulses to determine the force required to generate the target strain (5 με). Once this force value was obtained, five load impulses were applied. Finally, the five stiffness modulus values obtained were averaged. At the end of the test, the modulus values obtained and the diameter of the sample were checked. The test was discarded if the

modulus calculated along the second diameter differed from the first by more than 10% or less than 20%.

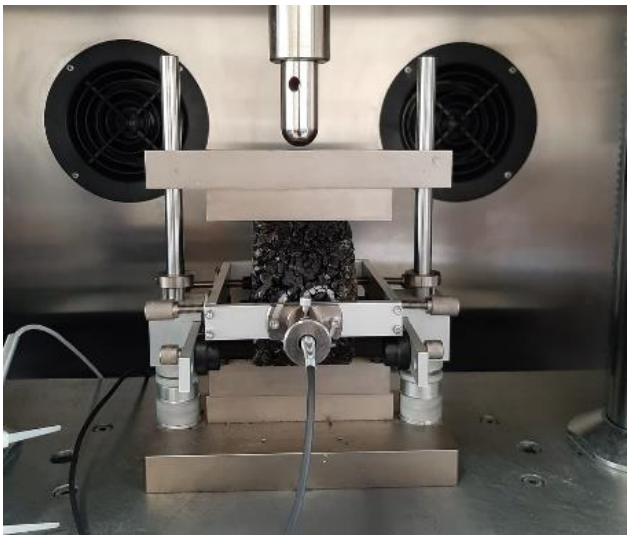

Figure 39. ITSM test equipment.

4.4 INDIRECT TENSILE STRENGTH TEST

The indirect tensile strength of cylindrical specimens was determined following EN 12697-23. The Samples were loaded diametrically until the break at specified test conditions. This procedure provides the performance at low temperatures of the different model systems.

The destructive test was developed in the UTM-30 machine, which allowed a constant deformation rate and accurately determined the load applied. Test instrumentation consisted of a small frame with a testing head equipped with loading strips of hardened steel having a concave surface. Figure 40 presents the ITS test configuration described by EN 12697-23.

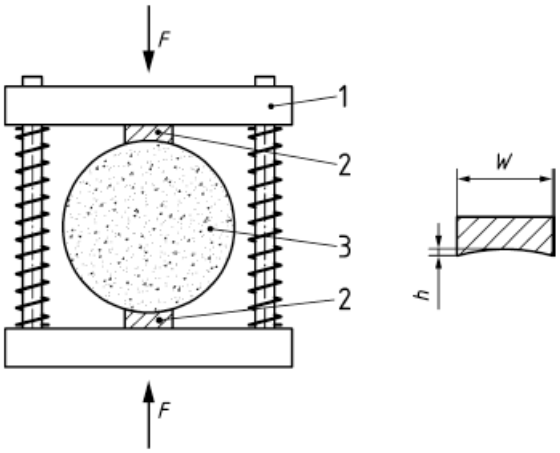

Key

1	testing head
2	loading strips
3	specimen
W	Width of the loading strip
h	Maximum height difference at the curved side of the loading strip
F	load

Figure 40. Testing head with loading strips. (EN 12697-23)

The cylindrical specimens tested of 65 mm height and 100 mm diameter were conditioned overnight at 4ºC, then placed in the compression testing machine between the loading strips and loaded diametrically along the direction of the specimens axis with a constant speed of displacement (50.8 mm/s) until it broke.

Figure 41. ITS test configuration

Figure 42. ITS sample break

The UTM-30 recorded time, axial force applied and the vertical displacement values. This data allowed the construction of the Force vs Displacement curve; Figure 43 is reported as an example of the curve for RA from source B.

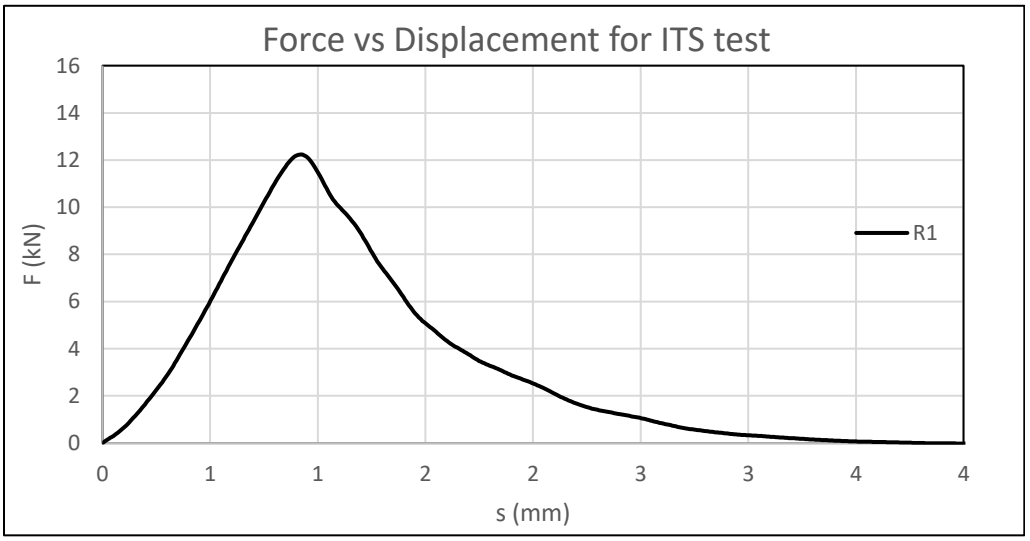

Figure 43. Force vs Displacement for ITS test

The indirect tensile strength is the maximum tensile stress calculated from the peak load applied at break and the dimensions of the specimen, as is presented in the following equation:

$$ITS = \frac{2\,F}{\pi \cdot D \cdot H} \cdot 1000$$

Where,

ITS is the indirect tensile strength (kPa)

F is the peak load (N)

D is the diameter of the specimen (mm)

H is the height of the specimen (mm)

In the following pictures, three examples of split samples are presented.

Figure 44. Samples after ITS

5. ANALYSIS OF RESULTS

In this chapter, all the results obtained from the experimental tests explained before are presented and analyzed. First, the outcomes achieved from the volumetric characterization of the compacted samples are reported, and then the results of the various mechanical tests performed.

5.1 CHARACTERIZATION OF COMPACTED SAMPLES

After the characterization of RA from B, C and S sources was realized, the compaction of the samples for the three MS types (Black, Rejuvenated and White) was executed. It was analyzed the number of gyrations, the self-compaction (C1), workability (k), the density of the sample, air voids content, and the most critical parameter to check, the VMA. According to the definition of MS, the Voids in Mineral Aggregates target was 30±1%. In the section Attachments, the sample characteristics for both sizes (100 or 65 mm height and 100 mm diameter) are presented. Therefore, it can be verified that VMA values for all sources MS are close to the target.

The average values of workability k, self-compaction C1 and the number of rotations performed by the gyratory compactor machine are evaluated. Then, it is possible to compare the percentage of binder effects and the Rejuvenating Agents' impacts in each source and finally make a general evaluation of the material.

Figure 45 compares the number of gyrations and the percentage of binder included in RA for all sources. It is represented with an equal dosage (8%) of Rejuvenating Agent for all RS to compare RA sources under the same conditions.

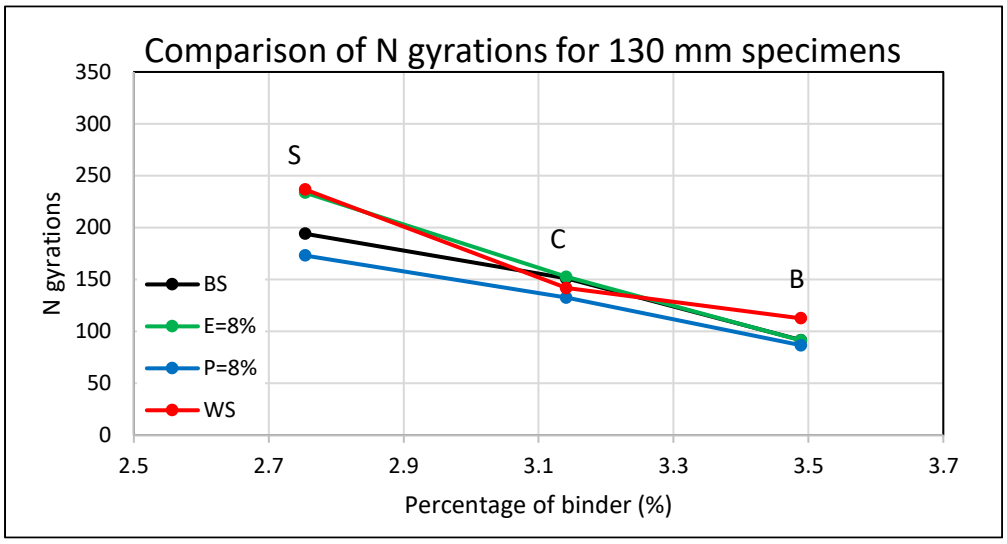

Figure 45. Comparison of the number of gyrations for the different sources using specimens of 130mm height

It is evident that a linearly decreasing trend characterizes the behaviour: higher the binder content is, lower the number of gyrations is. This tendency is due to the lubrication effect provided by the bitumen to the aggregates, as higher the binder content is, more lubricated the particles are.

As characterized before, the percentage of B, C and S binder content is different, but all MS of each source contain the same amount. Therefore, this condition shows that is greater the effect of the binder content than of the binder type.

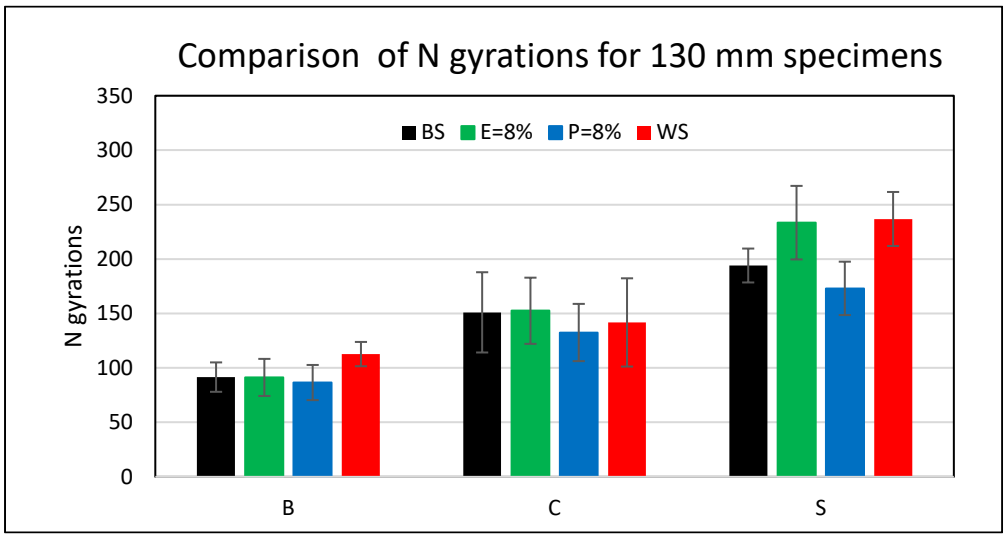

Figure 46. Comparison of the number of gyrations for the different sources using specimens of 130mm height, bar chart

Figure 47 presents the same comparison but uses the rejuvenated system with the optimum dosage of the Rejuvenating Agent. As explained later in the dynamic modulus test results analysis, the optimum dosage for B and S sources remains 8%. However, it varies for the C source, which is obtained 10.5% and 14.5% of the Rejuvenating Agent by weight of bitumen for E and P, respectively. Nevertheless, the change in the number of gyrations is not significant. Therefore, this analysis does not provide a clear advantage for the Rejuvenating Agents' employment, nor a difference between the types of Rejuvenating Agents, E and P.

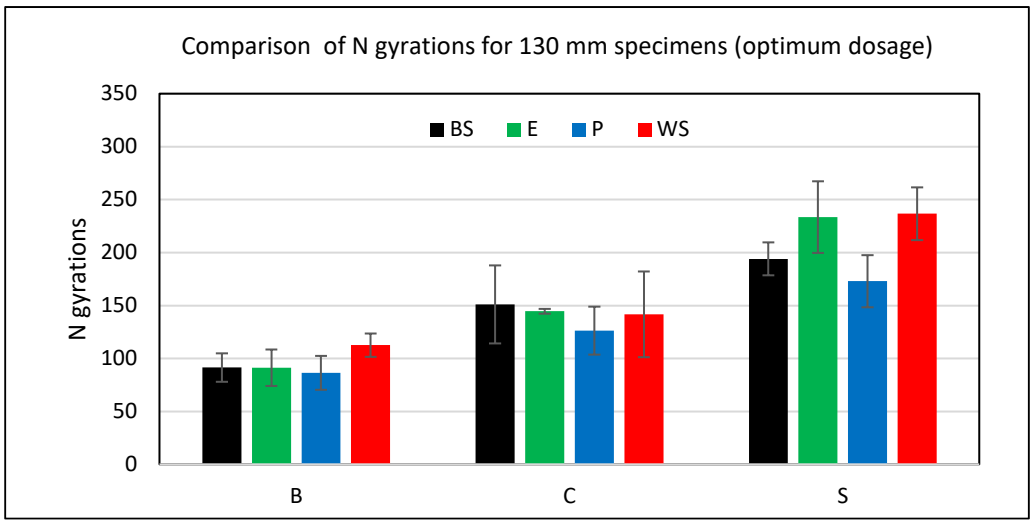

Figure 47. Comparison of the number of gyrations for the different sources with Rejuvenating Agent optimum dosage

Self-compaction C1is the value of the degree of compaction at the first gyration, representing the settlement by its own weight. It is closely related to the mixture's lithic skeleton and the size and shape of the aggregates. For all MS is assumed that the lithic structure is constant, making it possible to evaluate C1 versus the rejuvenating dosage without considering extra variables. Figure 48 presents all MS investigated in the current study.

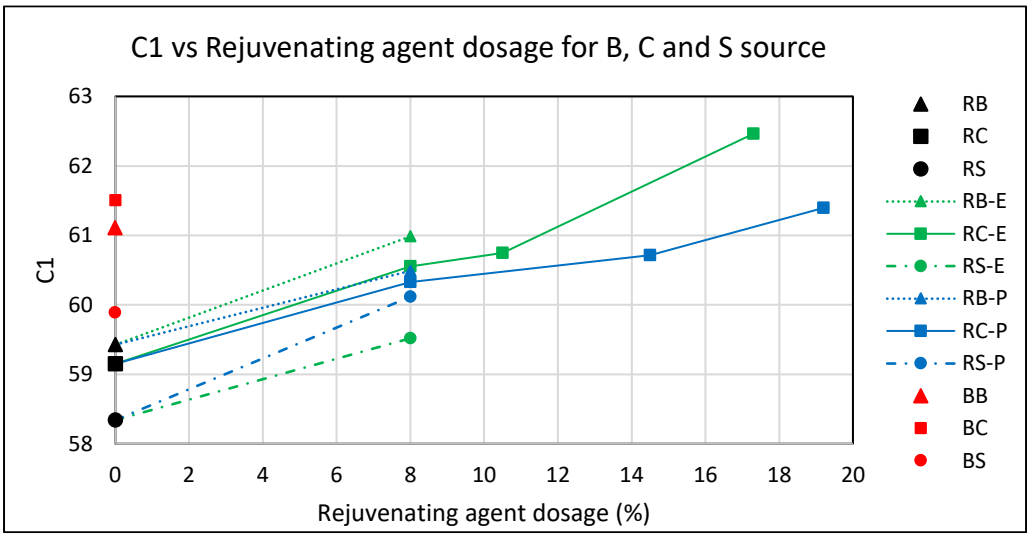

Figure 48. C1 evaluation for all sources with different Rejuvenating Agent dosages.

WS are characterized by high C1 values, opposite behaviour to BS with the lowest C1 values. For RS, instead, the increasing linear trend using E or P Rejuvenating Agent is clear for all RA sources. The behaviour that characterized WS and RS is attributed to the lower viscosity of the virgin and rejuvenated binder, respectively, that lubricates the aggregates and facilitates the self-compaction of the material. This behaviour evidenced that the Rejuvenating Agents regenerate the stiff binder and reduce its viscosity.

In the analysis, as higher the binder content in the 5/8 RA is, a higher value of C1 was obtained; this is also attributed to the increasing lubrication of the aggregates. Therefore, the material will self-compact faster with a thicker binder film because of its own weight, without any force applied. Furthermore, the particles will experiment less friction between each other if the cover film of the aggregates is softer, helping to accommodate the structure effortlessly, without having particle to particle touch.

The Attachments section presents the individualized figures C1 vs Rejuvenating Agent dosage for each source, where it can be easier to evaluate that using the optimum dosage of the Rejuvenating Agent, the C1 value is closer to the reference system (WS).

Workability is also obtained from the compaction curve. It represents the compaction gradient or, in other words, how easy is the compaction of the samples. Higher k will require fewer gyrations to compact the material. The particles are being forced to accommodate, applying a vertical pressure of 600 KPa.

Figure 49 shows the k values for all MS and as a function of the Rejuvenating Agent (E and P) dosage.

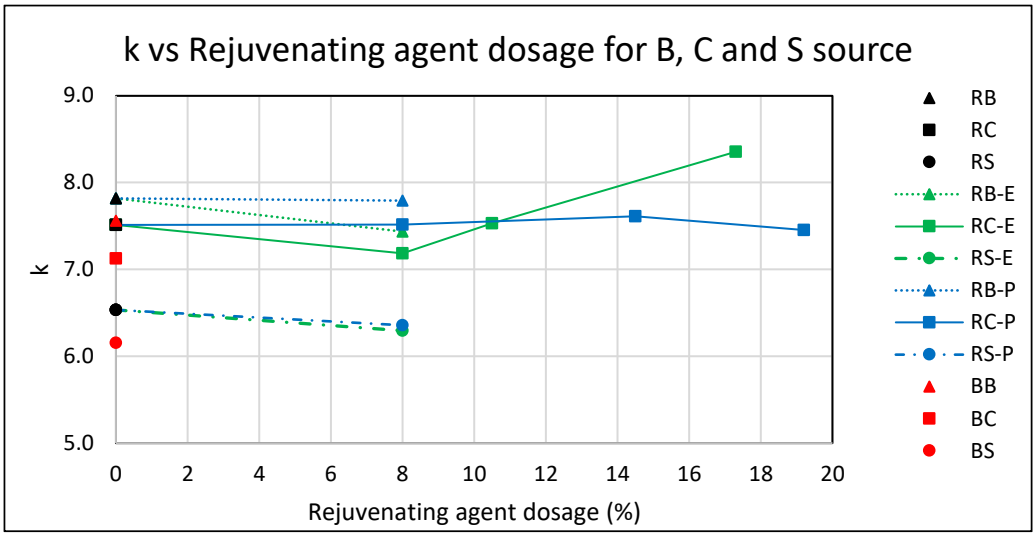

Figure 49. k evaluation for all sources with different Rejuvenating Agent dosages.

It is typical for cases where C1 was higher to present a lower k value. This trend is evident because the original material already underwent greater initial compaction, making it more challenging to continue the compaction process. Figure 49 also shows a constant trend for all rejuvenated systems with a dosage between 0% and 8% and not a clear trend for higher dosages values. The performance of Rejuvenating Agent P can be defined as constant, while for E, it continues to increase the k value with the addition of the Rejuvenating Agent. Concerning the additive P, the constant value of k can also be due to the black rock effect in which a portion of RA binder remains inert. For this reason, even when the vertical and horizontal forces are

applied during the compaction, the workability is not affected by the different amount P employed for such a RA.

It is also clear that the percentage of binder affects the workability. The higher is the binder content, the greater will be the workability. B, C and S are organized in decreasing order of %B and k values.

One more time, the results for each source are presented in Attachments, where it can be easier to analyze the effects of the Rejuvenating Agents. In particular, using the Rejuvenating Agent E at 8%, the workability in all RS is similar to the corresponding WS.

As a final comment about the compaction parameters, C1 and k, it can be said that the Rejuvenating Agent effects are more evident for C1 and that using the optimal dosage, the Rejuvenating Agent is capable of returning the aggregate lubrication, providing parameters close to WS.

5.2 DYNAMIC MODULUS TESTS RESULTS

After the post-processing of the raw data, the dynamic modulus and phase angle master curves were computed, representing the mechanical behaviour of the material at different temperatures and frequencies. Then the analysis of the linear viscoelastic behaviour of each MS was performed. The master curves are presented on the bi-logarithm plane. On the abscissa axis is the reduced frequency fr (Hz), while on the ordinate axis is the dynamic modulus | E * |. The reduced frequency was obtained by multiplying the load frequency by a factor called the shift factor, which is a temperature-dependent parameter.

As explained in the chapter on the methodology of testing, the master curves were a powerful tool to estimate the viscoelastic properties of each MS and define the optimum dosage of each Rejuvenating Agent.

First, the master curves for all BS and WS from the different sources were compared.

From BS, all three sources have close dynamic modulus results. However, C is the stiffer source, presenting the highest dynamic modulus, mainly due to the more severe ageing condition that characterized the material itself. Moreover, the coarser particles size could affect |E*| than other sources in which the particles' dimension is close to each other.

For the evaluation of WS, it is important to recall that all systems used the same 50/70 neat binder. The different behaviour between the B and C sources from the S supply is evident. B and C have close master curves; it is analyzed that they have similar air voids content, but C has a coarser granulometry condition that allows the modulus increment. S is characterized by low binder content, a high percentage of air voids and fine aggregates, attributes that reduce the system's stiffness.

The different curves shape between BS and WS were also compared. As explained before, the master curves are limited between two horizontal asymptotes: the upper, defined at low temperatures as a function of the binder limiting stiffness, and the lower, at warm temperatures, mainly influenced by the solid skeleton composition. The dynamic modulus obtained in both cases are very similar for the low temperatures. However, WS achieves lower dynamic modulus values for the high temperatures because of the reduced binder stiffness covering the aggregates.

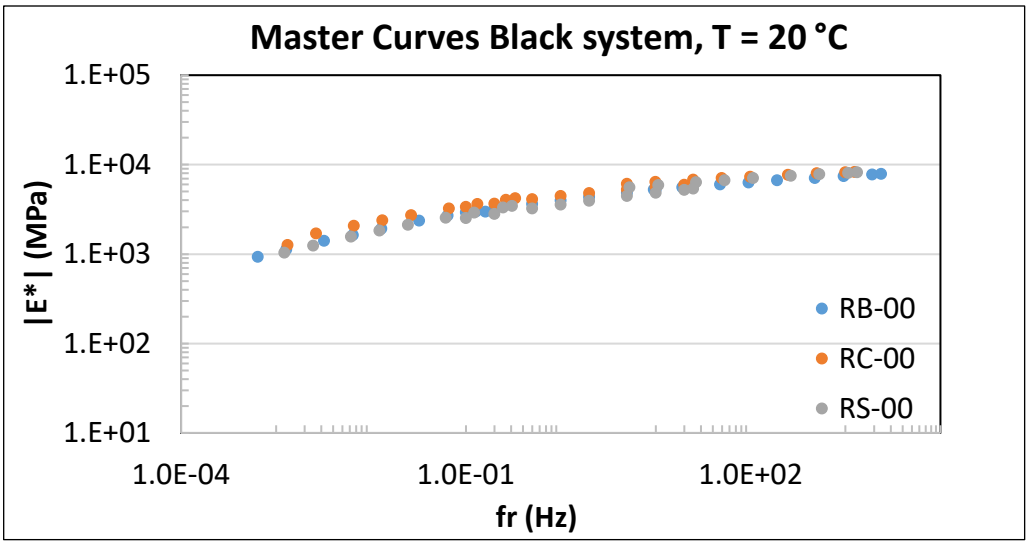

Figure 50. Black system master curves

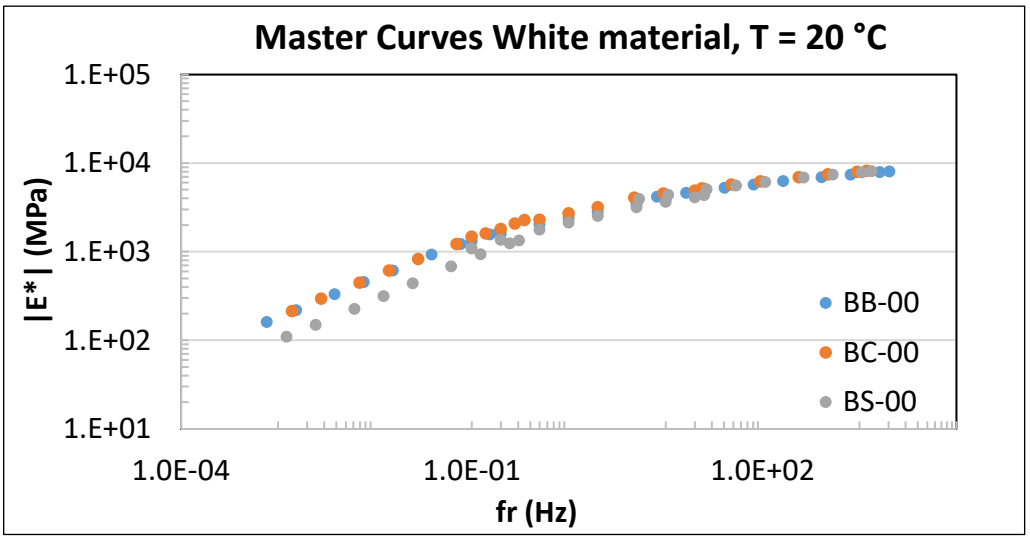

Figure 51. White system master curves

Next, the selection of the optimum dosage of the rejuvenated system for each source is presented. Previous investigations developed in the Road Materials Laboratory of Politecnico di Torino selected 8% as the optimum dosage for a different RA source, not included in the present thesis. Therefore, it was decided to impose as a starting point the value of the previous investigations and evaluate for B, C and S if the 8% achieved the requirements to be selected as the optimum dosage, or if it was required to evaluate a different Rejuvenating Agents' dosage.

The first source evaluated is B. After assessing the dynamic modulus of MS, the master curves were computed. As expected, BS has the higher |E*| due to the aged and stiff binder, and the lowest dynamic modulus is achieved by WS, imposing the reference values that RS must achieve. As presented in Figure 52, the master curves using 8% of Rejuvenating Agents overlaps WS for the medium and low temperatures. This means that the 8% may correspond to the optimal dosage.

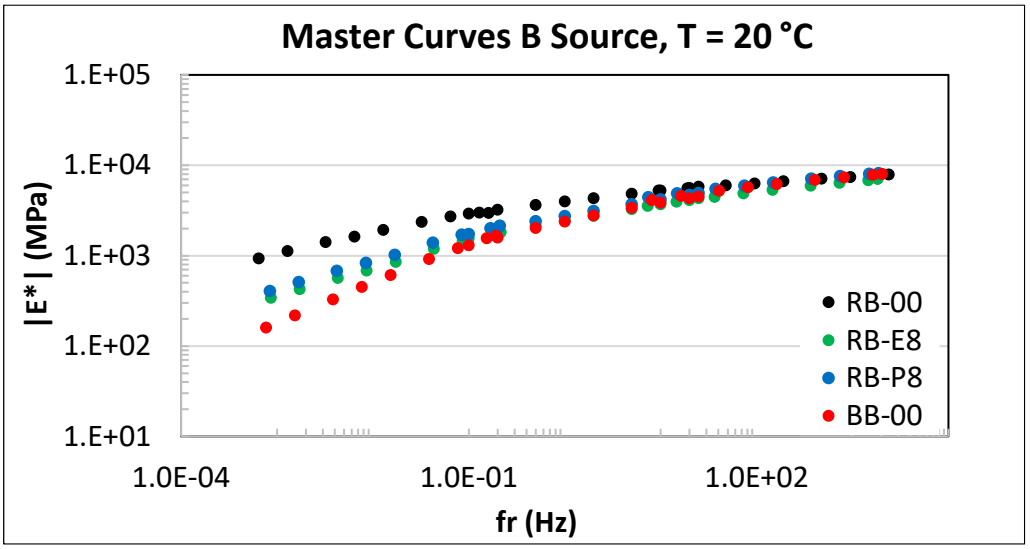

Figure 52. Master Curves for B source, optimum dosage

The ratio of the modulus obtained for BS and RS over WS versus the dosages evaluated was graphed to verify the optimum dosage value for all sources. 0% dosage corresponds to BS, while the other dosages to RS. The response was evaluated at 10 and 1 Hz, at 20ºC. The overlap of the results must be obtained to define the optimal dosage because they correspond to the intermedium frequencies.

It is defined as a rule to accept the Rejuvenating Agent dosage as the optimum, the ratio of RS evaluated, and WS for both frequencies (10 and 1 Hz) must be between 1 and 1.2. They are accepted stiffer RS than WS but not softer.

Figure 53 presents the verification for the B source, where it is evident that the results are in the established range, except the RB-E8 at 10 Hz.

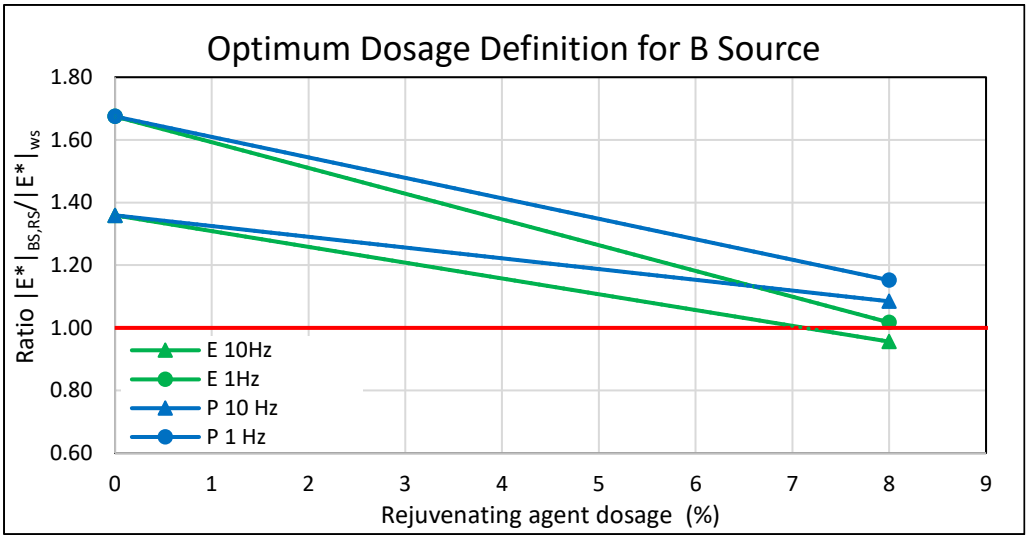

Figure 53. Optimum dosage definition for B source

To be precise, Table 6 presents the optimized dosages for each reduced frequency of the Rejuvenating Agents and the computed average.

Table 6. Verification of the optimum dosage for B source

Rejuvenating Agent for B	Y=1 (10 Hz)	Y=1 (1 Hz)	Average	Selected
	(%)	(%)	(%)	(%)
E	7.12	8.21	7.67	8.00
P	10.46	10.32	10.39	8.00

For E, the results for the optimal dosage was 7.67% by weight of bitumen, very close to 8%, the dosage already evaluated. Because of this proximity, a second dosage is not evaluated. On the other hand, even though the results for P are approved, the possible second dosage can be used to achieve a ratio closer to 1, meaning having closer properties to the reference system.

The second 5/8 RA source to be evaluated is S. Following the same abovementioned procedure, the 8% by weight of bitumen was the optimum dosage for this RA because of the good overlapping of RS and WS, but also because the verification rule was passed for both

Rejuvenating Agents, having a ratio higher than 1, but lower than 1.2. One more time, they have presented the possible second dosages values in case that it is decided to be more strict on the results.

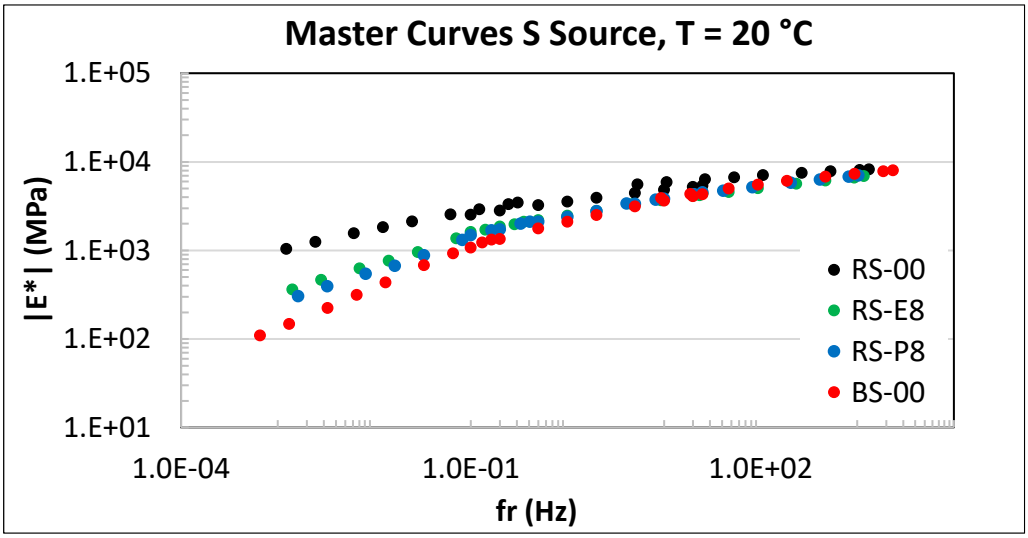

Figure 54. Master Curves for S source, optimum dosage

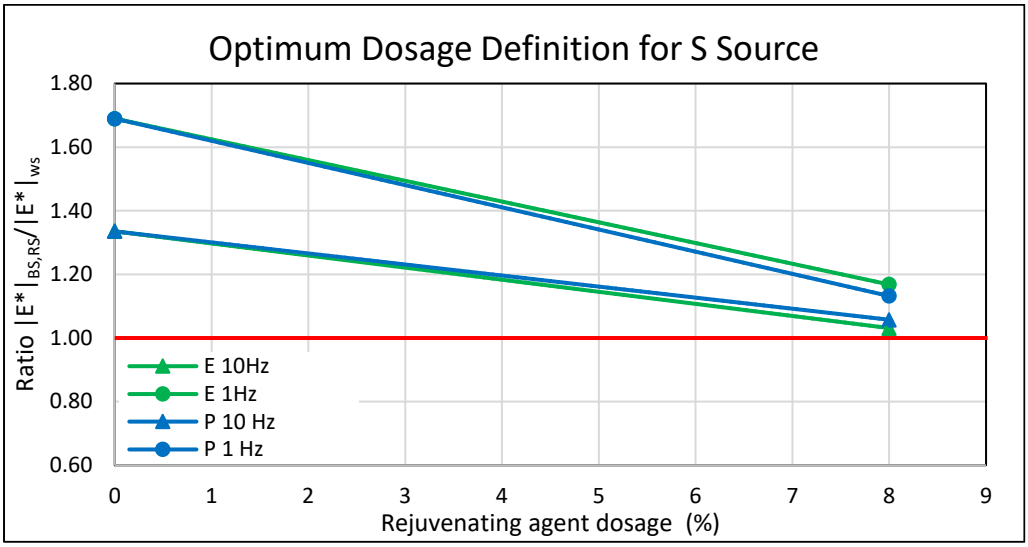

Figure 55. Optimum dosage definition for S source

Table 7. Verification of the optimum dosage for B source

Rejuvenating Agent for S	Y=1 (10 Hz)	Y=1 (1 Hz)	Average	Selected
	(%)	(%)	(%)	(%)
E	8.81	10.59	9.70	8.00
P	9.64	9.89	9.77	8.00

The third source to be evaluated is C. Figure 56 presents the master curves using 8% of Rejuvenating Agents. For this case, it is evident that this dosage is insufficient to obtain the required mechanical characteristics because RS and WS master curves are far from each other.

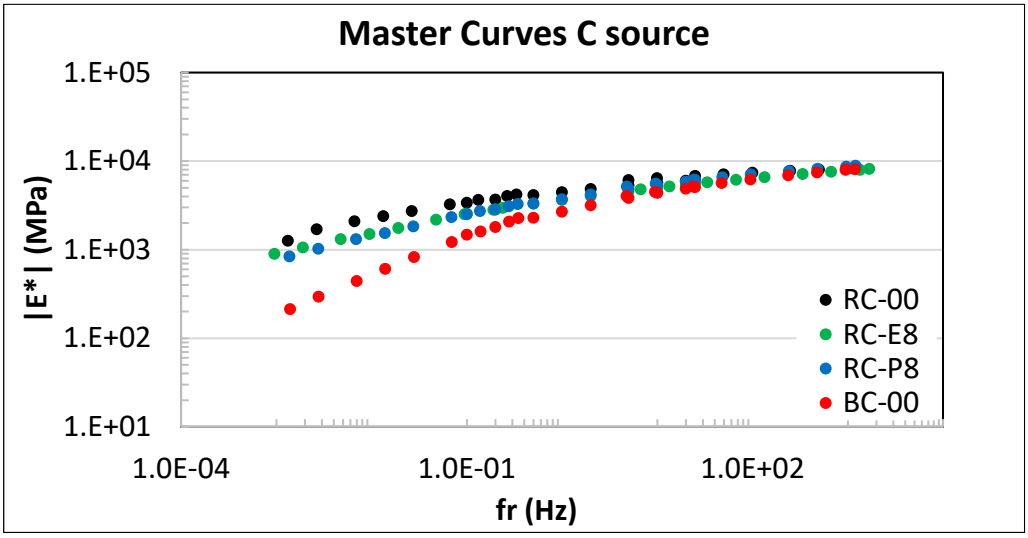

Figure 56. Master Curves for C source, 8% of Rejuvenating Agent

The dynamic modulus ratio graph verified what was expected; the ratios are out of the specified range, obtaining values higher than 1.2. Therefore, looking for a ratio equal to one were obtained high values of the Rejuvenating Agent dosage. Furthermore, it allows characterizing the C source with a RA older and stiffer than B and S because it requires more additive to achieve linear viscoelastic properties closer to the reference system (WS), verifying what was said before in the comparison of the master curves for BS.

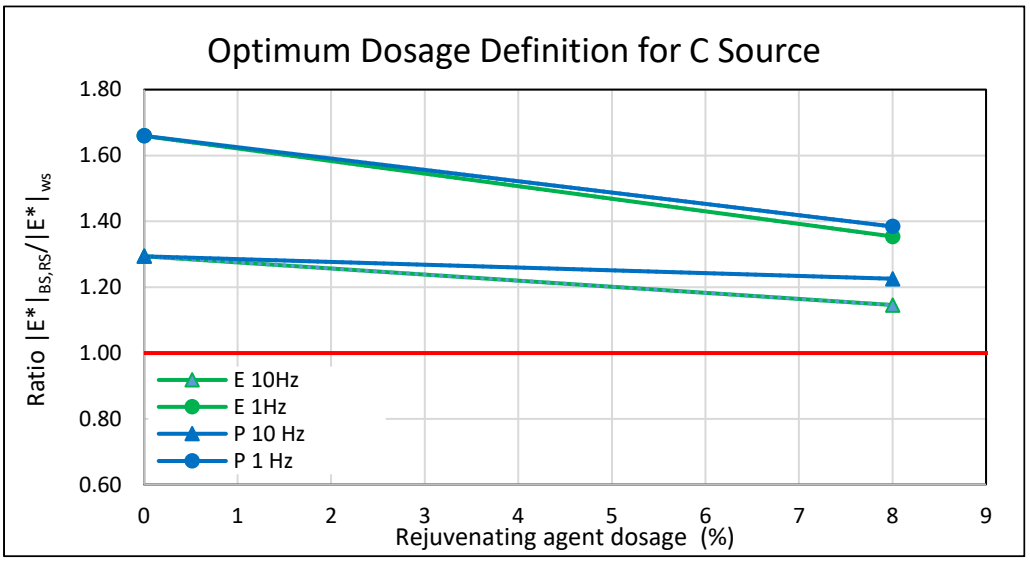

Figure 57. Optimum dosage definition for C source (I step)

It was selected for E and P as a second dosage, 17.3% and 19.2%, respectively, as computed for 1 Hz.

Table 8. Computation of the second dosage for C source

Rejuvenating Agent for C	Y=1 (10 Hz) (%)	Y=1 (1 Hz) (%)	Average (%)	Selected (%)
E	15.89	17.27	16.58	17.30
P	34.17	19.18	26.68	19.20

A new set of master curves were obtained with the new dosage of E and P and represented in Figure 58.

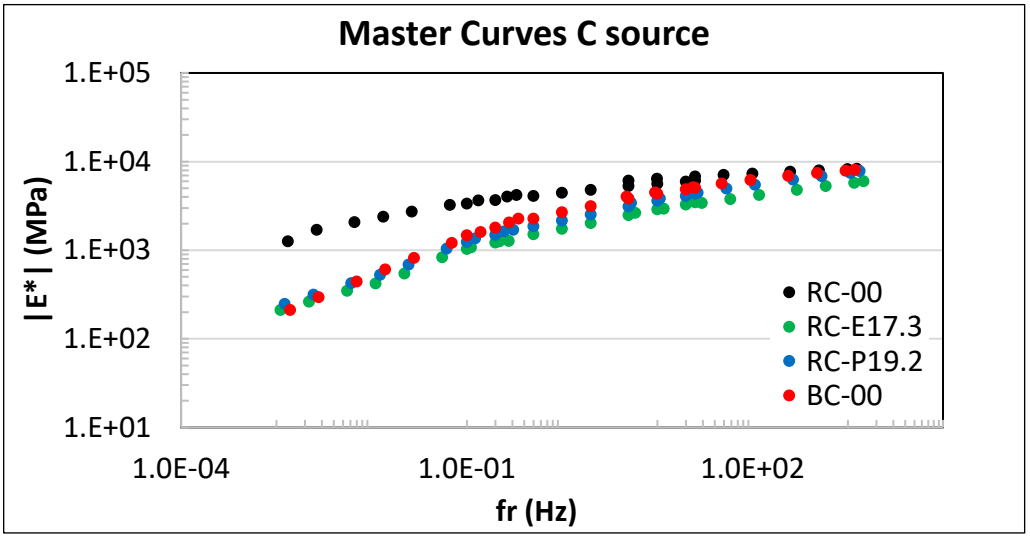

Figure 58. Master Curves for C source, 17.3% and 19.2% of Rejuvenating Agent for E and P

RS overpassed WS, meaning that the Rejuvenating Agent was used in excess and the obtained material was too soft, achieving ratio values lower than 1. These results were used to have new points in the dynamic modulus ratio graphs and compute the third dosage for the C source, 10.5% for E and 14.5% for P, as presented in Table 9.

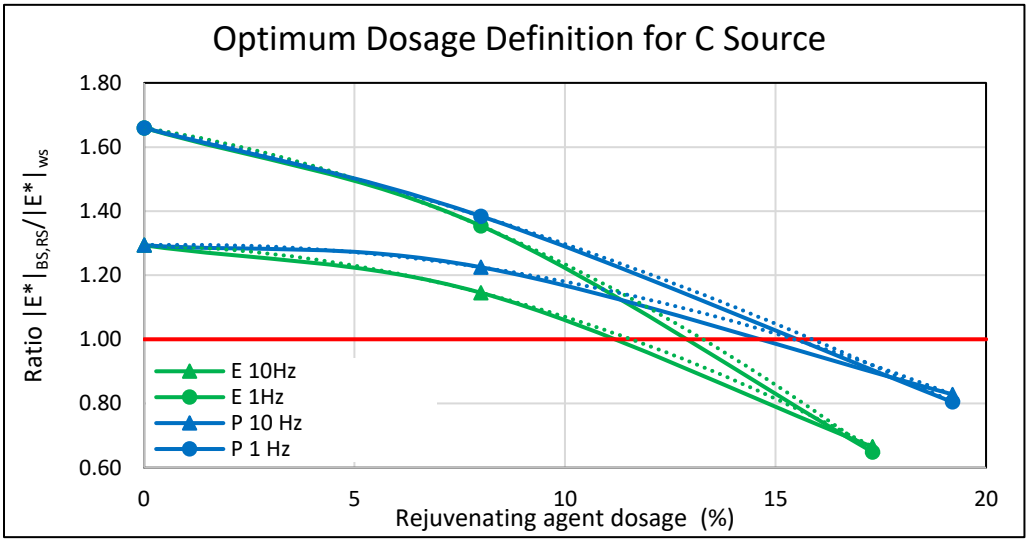

Figure 59. Optimum dosage definition for C source (II step)

Table 9. Computation of the third dosage for C source

Rejuvenating Agent for C	Y=1 (10 Hz)	Y=1 (1 Hz)	Average	Selected
	(%)	(%)	(%)	(%)
E	11.62	13.22	12.42	10.50
P	15.45	15.90	15.67	14.50

Computing the master curves and the dynamic modulus ratio graphs for the third dosage, it was verified that 10.5% and 14.5% by weight of bitumen are the optimum dosages for E and P Rejuvenating Agents, respectively. Furthermore, Figure 60 shows that RS overlap WS at low and medium temperatures and are close enough for the high ones. While Figure 61 verifies that the rule is achieved for the optimum dosage implemented, less for E at 10 Hz. Moreover, it is clear that the optimum dosage is elevated, being not economically feasible. Therefore, it must be considered the convenience of using or not this RA in future pavement constructions.

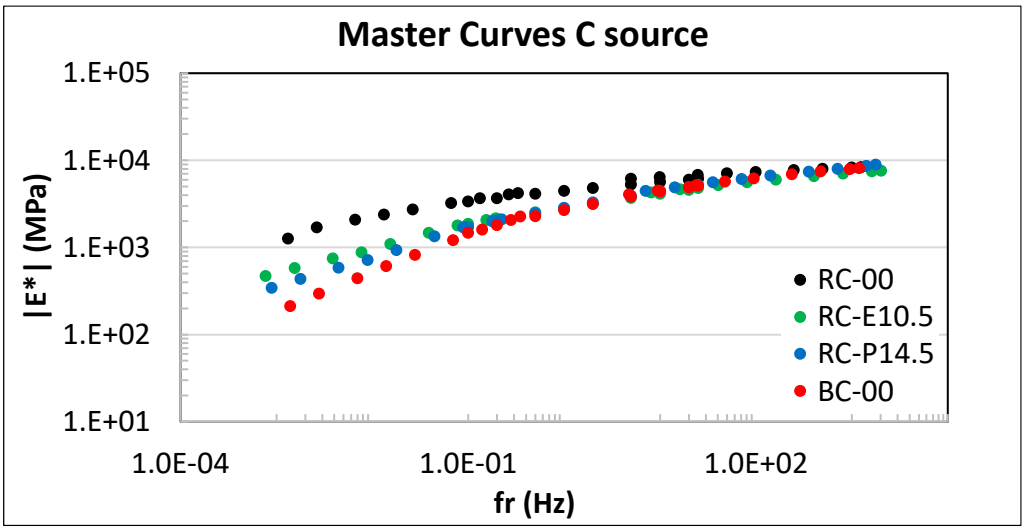

Figure 60. Master Curves for C source, optimum dosage

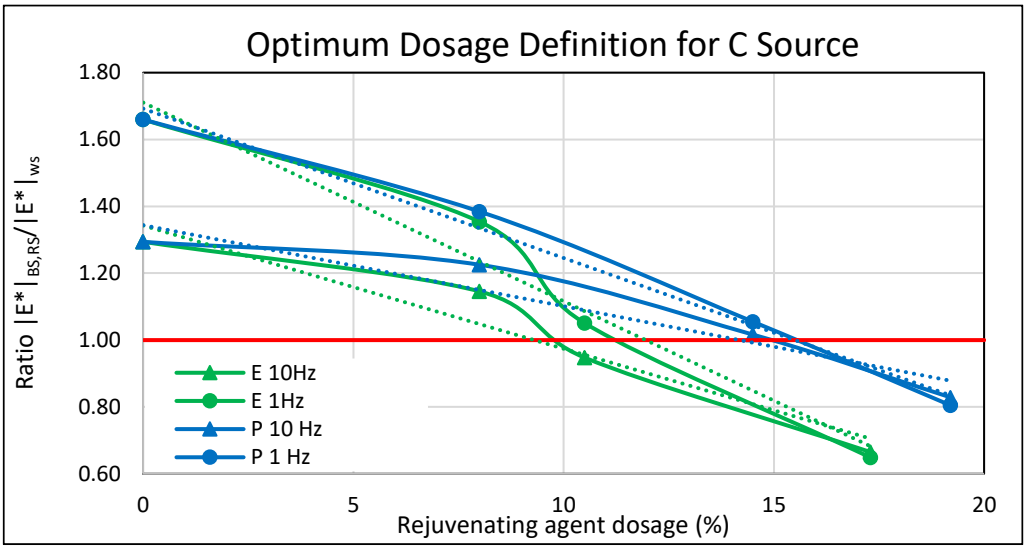

Figure 61. Verification of optimum dosage definition for C source

Figure 62 presents all the different dosages studied for the C source, which exemplify that if Rejuvenating Agent content is too low or too high does not actually regenerate the bitumen or exerts an exaggerated softening action, respectively. It is also evidenced that the |E*| decrease as the dosage increases; this is because of the softening action of the Rejuvenating Agents on the stiff binder, changing the rheological characteristics.

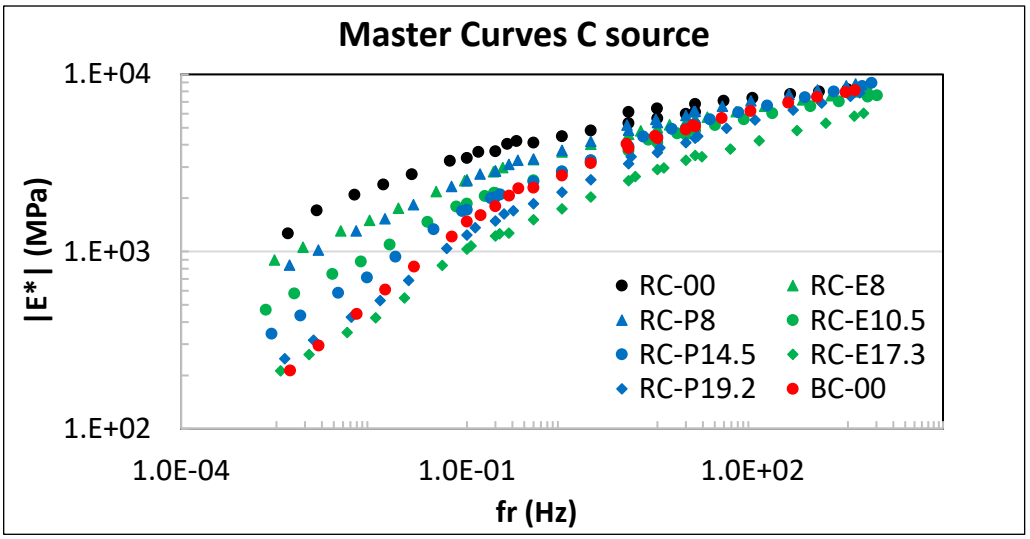

Figure 62. Master Curves for C source, all dosages studied

It is analyzed that always Rejuvenating Agent E requires a lower dosage than P. Furthermore, for 10 Hz, a lower amount of the additive is necessary than at 1 Hz; this is because, at lower temperatures, the overlapping of the curves is better than at high temperatures.

5.3 INDIRECT TENSILE STIFFNESS MODULUS (ITSM) TEST RESULTS

As said before, the ITSM test's primary objective in the present thesis is to analyze if its results for BS and WS were correlated to the dynamic modulus test outcomings, using the same materials but different geometry.

One of the goals of studying this relationship was to permit the characterization of the stiffness by alternative tests, allowing the classification of performance using a smaller sample that requires half of the material compared to the sample used for the dynamic modulus test. Therefore, the samples employed in the ITSM have 65 mm in height and 100 mm in diameter. This advantage reduces the amount of materials and sample preparation time. Other advantages are the common machinery employed and the simplicity of the computation of the results.

Table 10 presents the results for BS and WS for all loading times evaluated at 20ºC. Again, it is important to highlight that the diameter was checked after each test and did not show significant variations.

Table 10. ITSM results for BS and WS

			E (MPa)					
			RB-00	**BB-00**	**RC-00**	**BC-00**	**RS-00**	**BS-00**
Loading time	**(ms)**	**50**	4809	3587	5943	3848	3450	2685
		100	4293	2843	5630	3138	2992	2122
		125	4390	2563	5067	2458	2876	1963
		150	3888	2628	5122	2697	2752	1887
		200	3807	2380	4254	2566	2560	1707

Figure 63represents the results at 125 ms, making the difference between the systems evident.

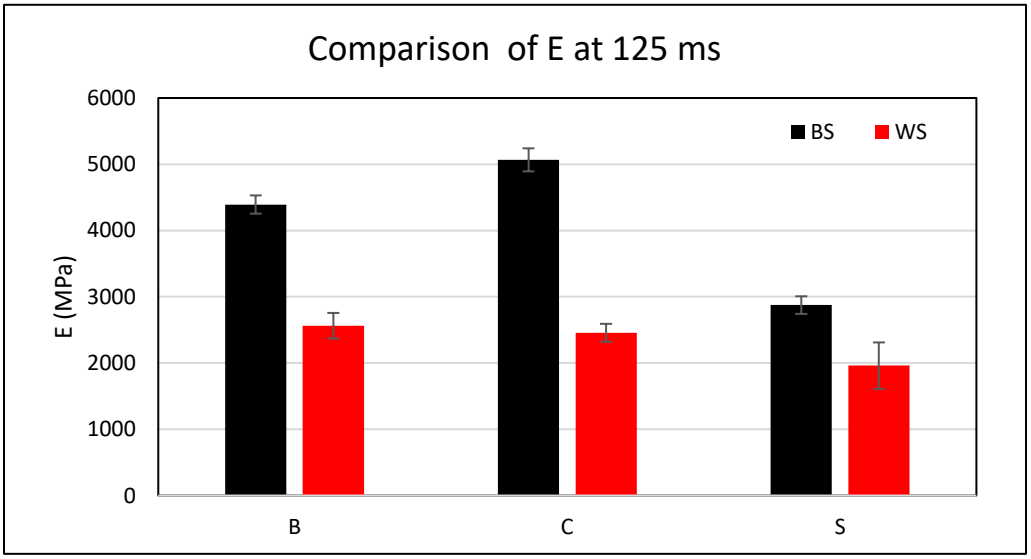

Figure 63. ITSM comparison results for 125 ms

It is clear that, in general, for all WS, the dynamic modulus is close to each other because they used the same 50/70 neat bitumen, proving that the binder phase mainly characterizes this test due to its indirect tension configuration. Nevertheless, the S source presents a slight deviation characterized by the lower binder content (2,8%); it is analyzed that having less binder requires less force to generate the same elongation. The possibility of the white granulometry affecting the results was also studied, but the white curves are pretty close between all sources.

For BS case, much higher values are obtained in confront to WS; the reason is that a much stiffer binder characterizes the system. Furthermore, one more time is evidenced that RA from source C has the highest modulus value; the main reason is that it is composed of the stiffest binder and the coarser RA. Again the percentage of binder content in S affects its behaviour.

Figure 64, 65 and 66 are used to analyze the change of the dynamic modulus in function of the loading time.

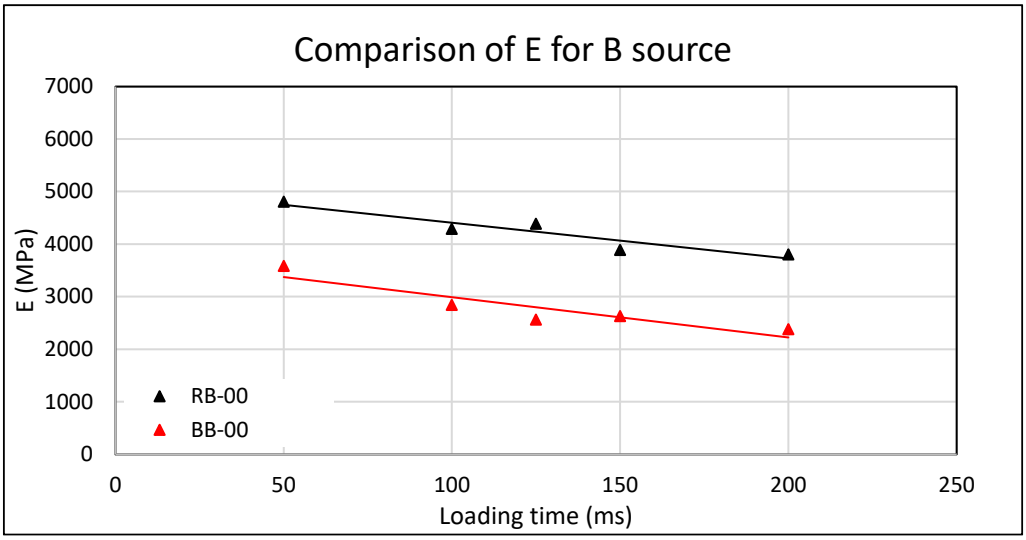

Figure 64. ITSM results for B source

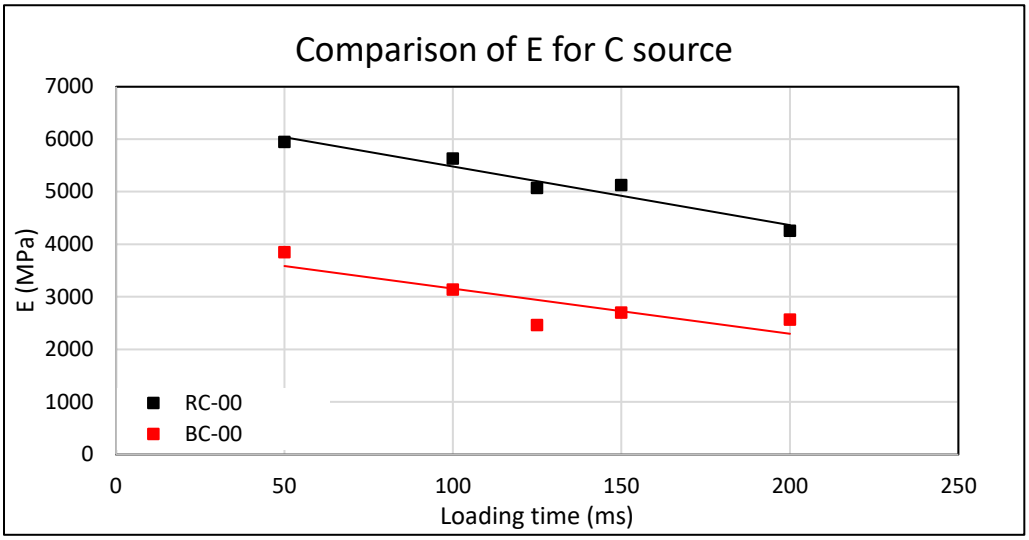

Figure 65. ITSM results for B source

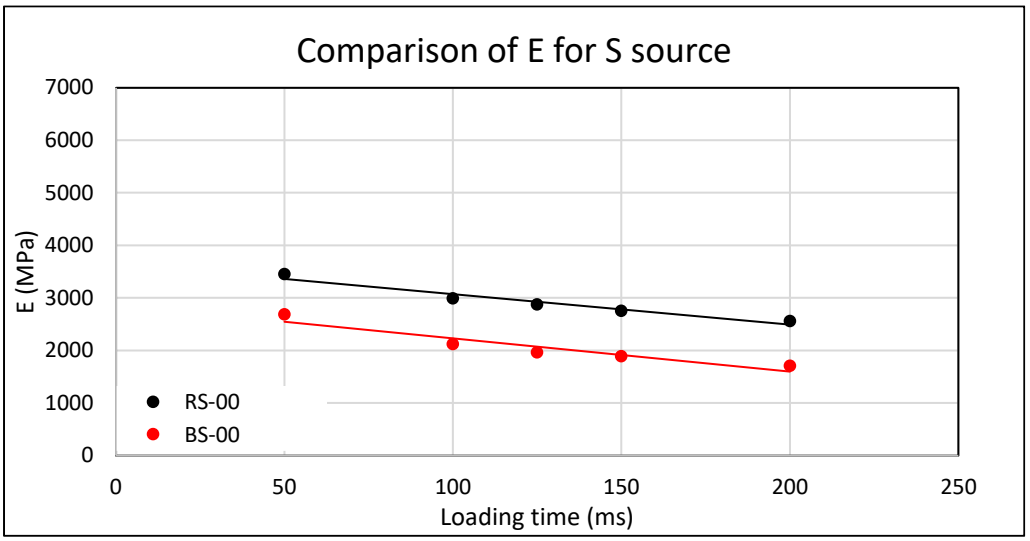

Figure 66. ITSM results for B source

First, it can be established that for all MS, the behaviour follows a decreasing trend that could be approximated with a linear trend. Also, the stiffness reduces as function of the rise time or loading time, similar to the concept of |E*| vs reduced frequencies discussed with the dynamic modulus master curves. These figures represent a piece of a pseudo master curve if the conversion to the loading time into reduced frequency is realized.

Once the linear interpolation of ITSM results was defined, the slope and the distance between BS and WS were analyzed. The higher slope value for both systems is obtained for the C source, characterizing the material as the most sensitive to loading time. As already established, this material is the coarsest and has less air voids content, which may affect the sensibility to loading time. On the other hand, the ageing of this RA does not affect the slope because WS, which includes the virgin binder, is also characterized by a high slope.

To study the difference in the distance between BS and WS, the ratio among the systems' dynamic modulus is presented in Figure 67.

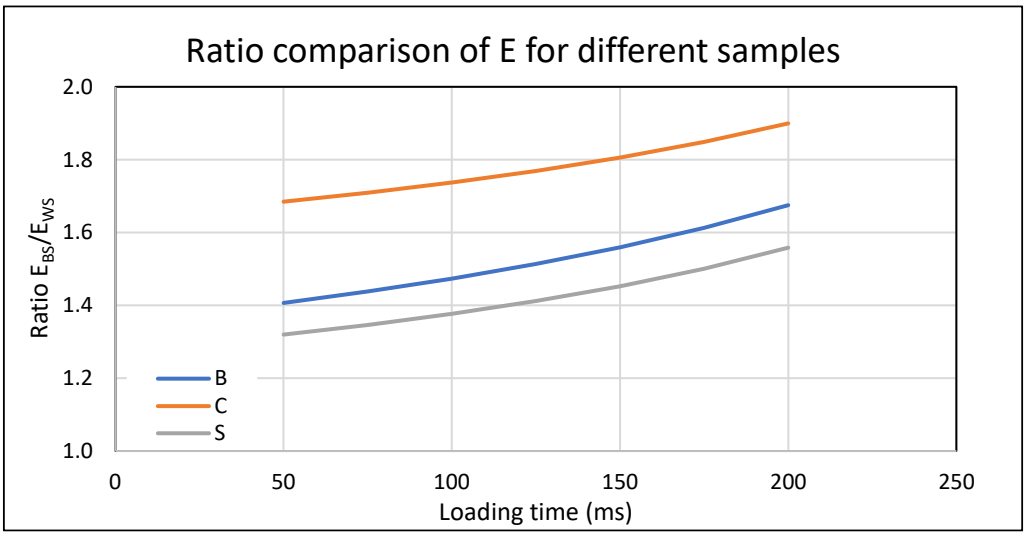

Figure 67. Ratio comparison between BS and WS

Considering that all WS are made of the same 50/70 neat binder, this ratio can be taken as an ageing index of the binder phase, independent of the percentage of binder content or the lithic structure, because for all MS of each source, these conditions are the same. Another not considered parameter is the compaction degree, since the number of gyrations is close for each source. This way, the ageing index compares how stiffer is the binder phase, respect to the reference conditions (WS).

If the ratio is equal to one, it will mean that the binder is not aged. The minimum value obtained is for S, corresponding to 1.3, and the highest for C source 1.9, meaning that, on average, the sources BS are 1.6 times stiffer than its reference system. As Figure 67 shows, the sources are organized as C, B, S in decreasing age.

Finally, the comparison between the dynamic modulus master curves and the ITSM pseudo master curves (by converting the loading time into frequency) are plotted for each source in figures 68, 69, 70, 71, 72 and 73.

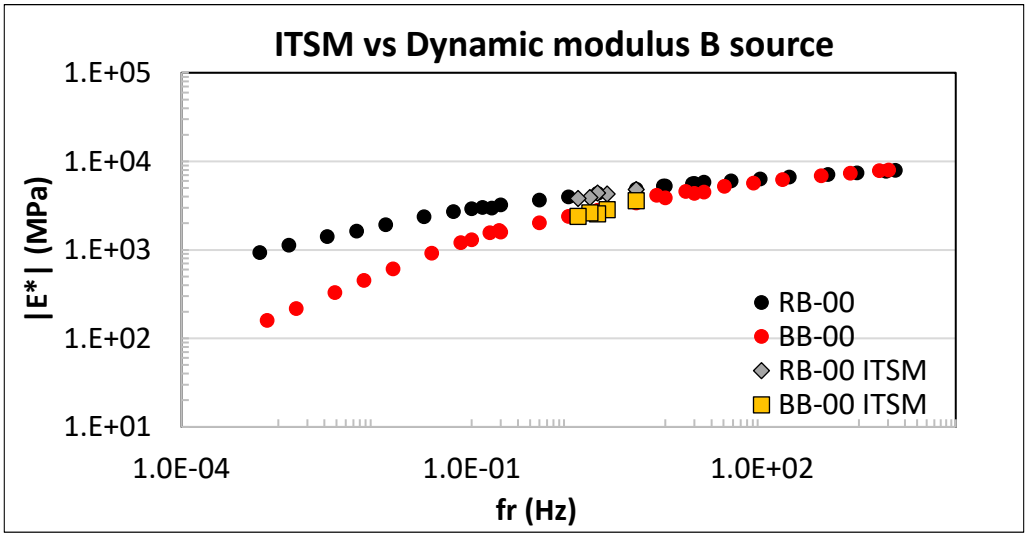

Figure 68. ITSM vs Dynamic modulus results for B source

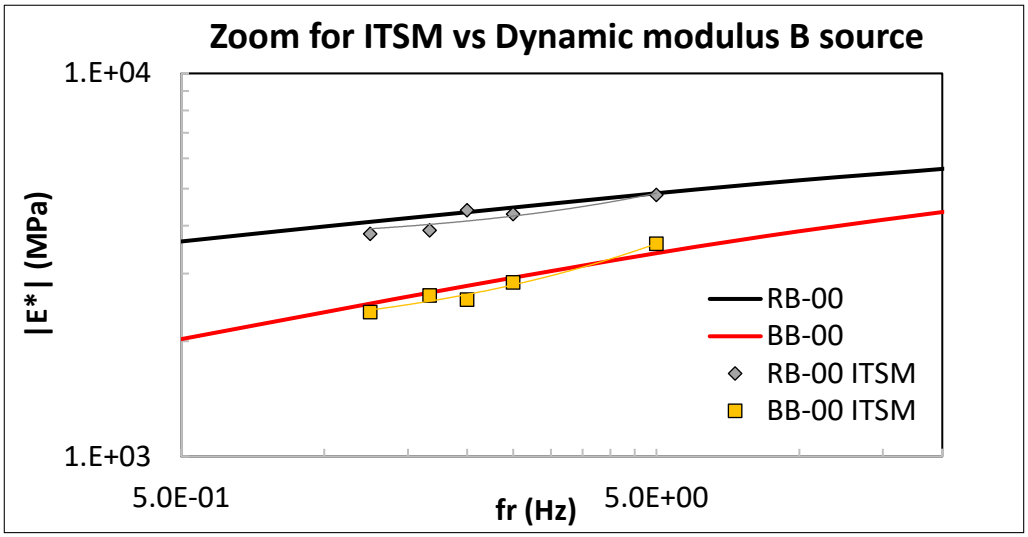

Figure 69. ITSM vs Dynamic modulus results for B source (zoom)

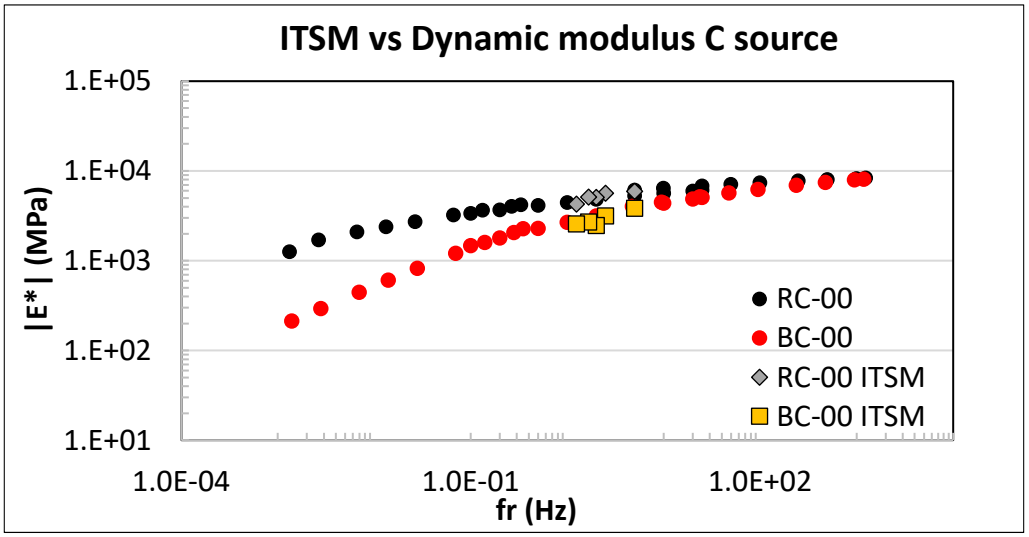

Figure 70. ITSM vs Dynamic modulus results for C source

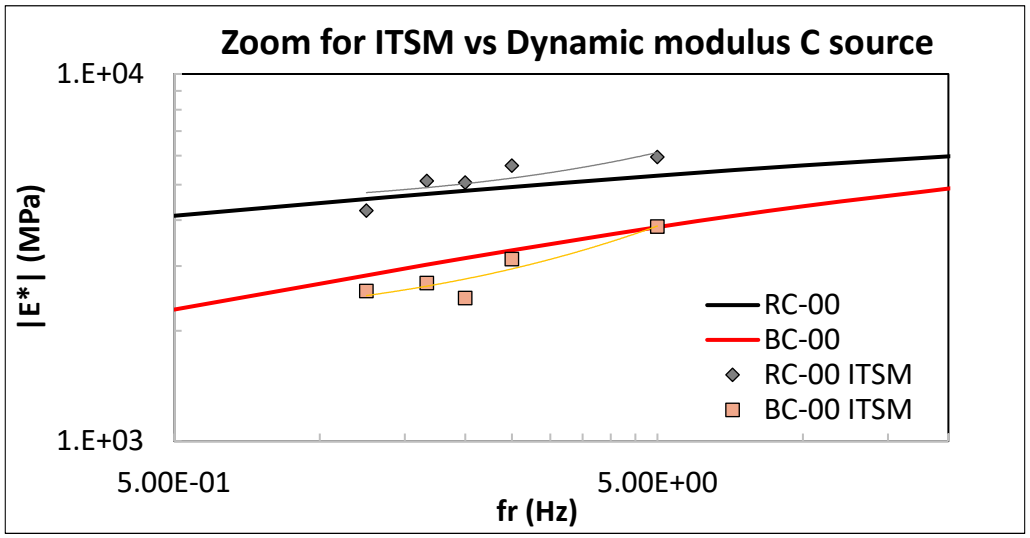

Figure 71. ITSM vs Dynamic modulus results for C source (zoom)

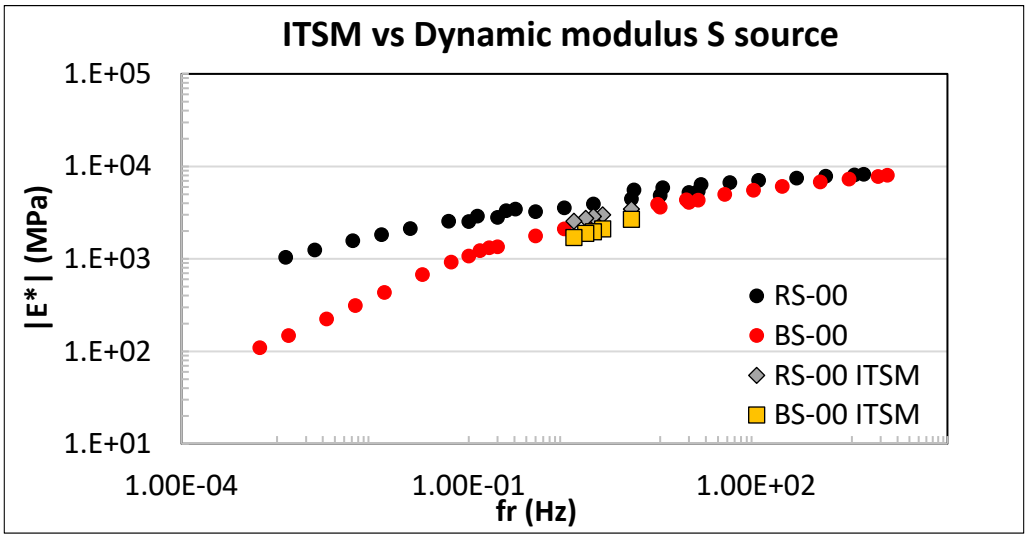

Figure 72. ITSM vs Dynamic modulus results for S source

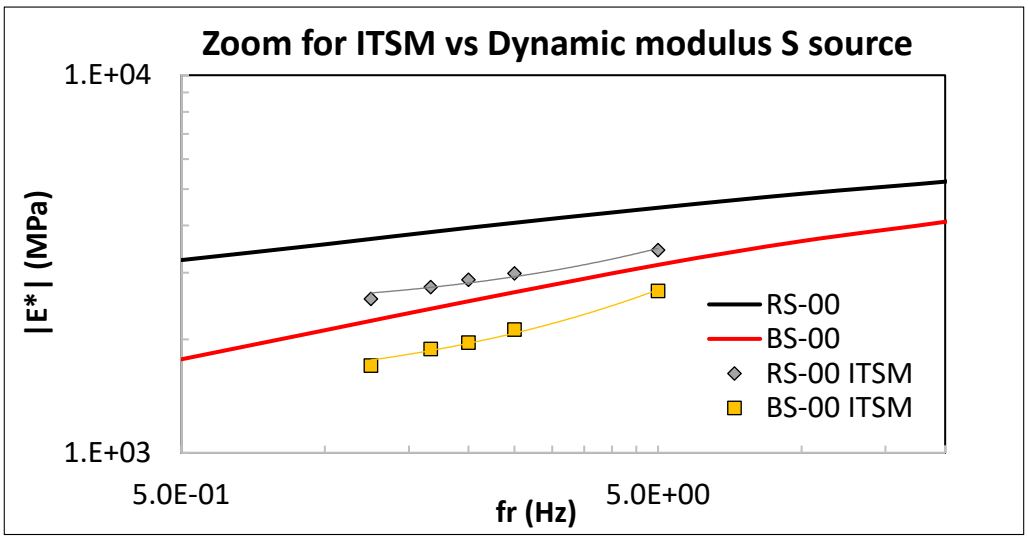

Figure 73. ITSM vs Dynamic modulus results for S source (zoom)

ITSM, as established, requires cheaper equipment and less material and the samples are tested by applying a haversine loading in indirect tension configuration. While the Dynamic modulus test employs an expensive and complex machine, also it is time-consuming; such a test applies a vertical sinusoidal loading in a compressive configuration. The results differences are attributed to the variations in the test configuration. Under sinusoidal loading compression, the results depend on the binder and aggregates response. In contrast, the ITSM test response is mainly dependent on the binder phase. Consequently, the expected modulus results are higher when compressive sinusoidal loading is applied than indirect tensile.

The three different BS and WS used in both tests are characterized by a constant VMA, similar lithic structure, but different binder content and percentage of air voids. Moreover, they were evaluated at the same temperature and frequencies obtained by converting the rise time into a frequency.

After the computation of the master curves, the results can be analyzed graphing ITSM vs Dynamic modulus results figures evidenced that for higher binder content, there is a correlation between both tests, but for lower binder content is not present this relationship. The reason may be that less force is required to generate the same elongation at low binder content. Therefore, it is established that the binder content is a limiting parameter for RA employed because of the different test configurations.

It can be recognized that MS that includes a percentage of binder higher than 3.1%, ITSM can predict a sample's dynamic modulus, obtaining pseudo master curves that matched quite well the ones obtained with the dynamic modulus test. Moreover, the overlapping between the master curves could be better with higher binder content.

The whole behaviour for WS, where the binder type is the same for all MS, is the primary explanation. The S source has the lowest binder content, equal to 2.8%. Consequently, its

particles are not glued properly, and the big difference between tensile and compression modulus is evident. Then, evaluating the C source, as RA is changed, and with it, the aggregates, and the binder content, 3.1%, but all other parameters remain equal, the addition of bitumen is considered an improvement of the glueing the lithic structure. It reduced the air voids, increased the voids filled with bitumen, made a more continuous system and consequently, the results started to overlap. Finally, the B source, characterized with the highest binder content, 3.5%, can verify the analysis, having the closest results for ITSM and dynamic modulus. The same behaviour was analyzed in BS but with the binder type additional variable.

Such a concept are clearly explained considering the graphical representation in Figure 74, in which the aggregates-bitumen interaction is represented in 2D configuration.

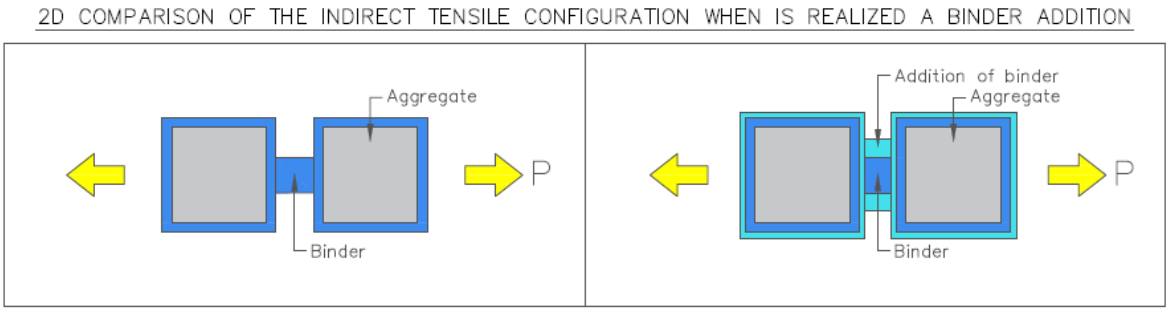

Figure 74. 2D comparison of the indirect tensile configuration when is realized a binder addition

Two aggregates covered by a thin binder film subjected to tension are presented on the left side. On the right side, instead, the same situation with the addition of a binder that covered both aggregates and increased contact point area is shown. In the right side condition, the force will be distributed in a greater area, and the stress carried by the bitumen will be lower. This connection with the extra binder is still weak because it is working in tension, but its strength will be higher than the one without the addition of the binder, generating a less deformable response. In the following expression, the behaviour is resumed.

$$\frac{P}{A_{glue\ reduced}} = Stress_{low\ binder\ content} > \frac{P}{A_{glue\ Increased}} = Stress_{high\ binder\ content}$$

It is clear that it must be considered if the same behaviour is observed in other materials and at other frequencies.

To evaluate in a numerical way how close are the results, it is made the ratio between the linear regression of ITSM results and the dynamic modulus master curve that followed the sigmoidal function. A range of acceptable overlapping results is established as the lower limit of 0.85 and the higher limit of 1.15. Table 11 presents the results, evidencing the ratio between the established range for RA source B for all the evaluated frequencies. For the C source, it can be said that almost all of the results are accepted. While for S, no results are in between the specified ratio. The ratio confirms what was analyzed before.

Table 11. Ratio comparison of ITSM results and |E|*

0.85<Ratio<1.15

	B = 3.5%B		C = 3.1%B		S = 2.8%B	
fr (Hz)	**Ratio RB-00**	**Ratio BB-00**	**Ratio RC-00**	**Ratio BC-00**	**Ratio RS-00**	**Ratio BS-00**
5.00	0.97	0.95	1.07	0.90	0.53	0.78
2.50	0.97	0.97	1.05	0.92	0.51	0.80
2.00	0.96	0.96	1.02	0.90	0.48	0.79
1.67	0.94	0.93	0.99	0.87	0.46	0.76
1.25	0.90	0.85	0.90	0.78	0.40	0.69

5.4 INDIRECT TENSILE STRENGTH TEST RESULTS

Samples with dimensions 65 mm high and 100 mm diameter, preconditioned at a temperature of 4 °C, are employed for the Indirect Tensile Test (ITS).

This test configuration is based on the indirect tensile strength. The responses obtained mainly correspond to the binder, which is glueing and keeping together RA and aggregate particles.

Figure 75, 76 and 77 and Tables 12, 13 and 14 have compared ITS (MPa), maximum displacement at break s (mm) and load F at the peak (kN) for all tested materials.

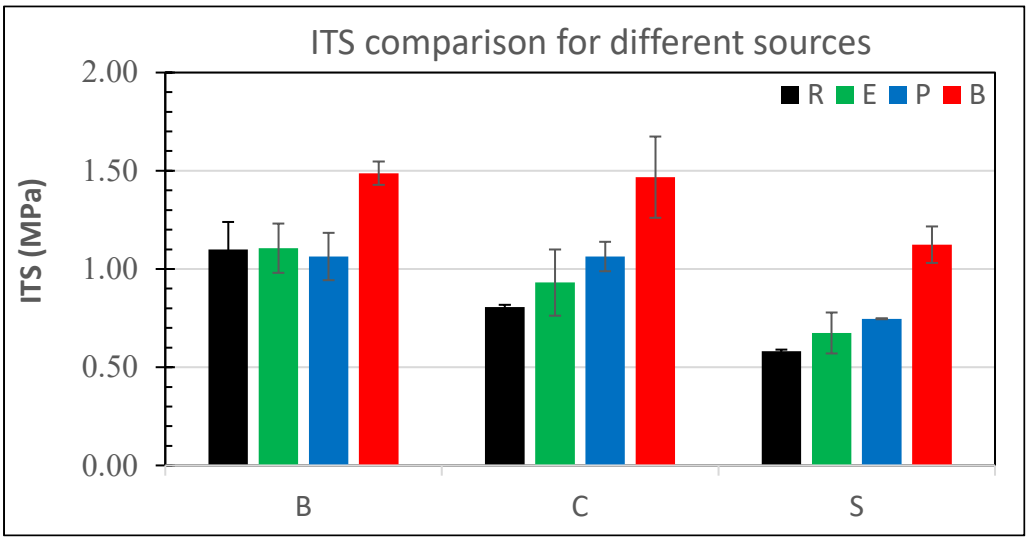

Figure 75. ITS comparison results for different sources

Table 12. ITS comparison results for different sources

	ITS (MPa)				dev.st (-)			
	R	**E**	**P**	**B**	**R**	**E**	**P**	**B**
B	1.099	1.106	1.063	1.487	0.140	0.126	0.121	0.060
C	0.807	0.931	1.063	1.467	0.010	0.168	0.075	0.207
S	0.581	0.675	0.747	1.124	0.009	0.104	0.002	0.093

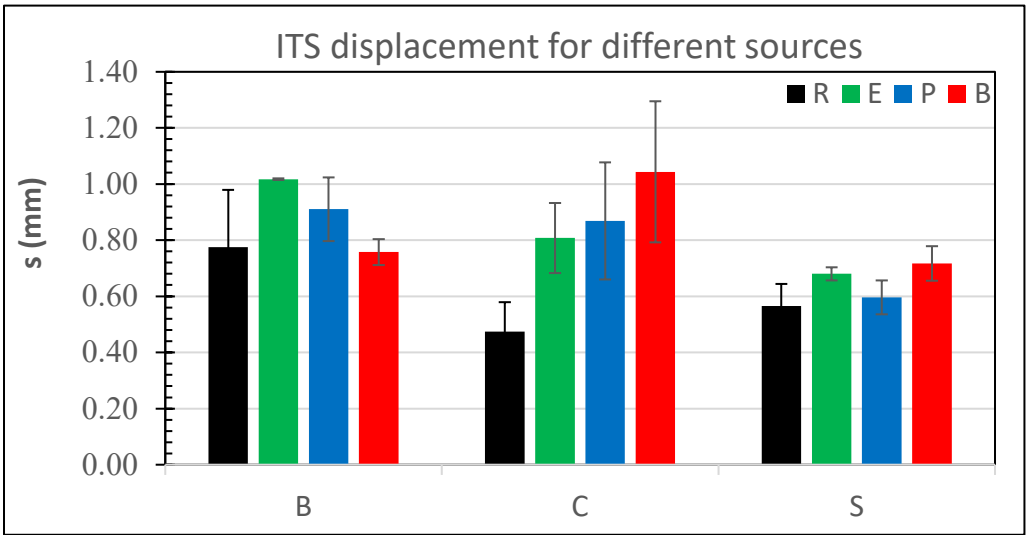

Figure 76. ITS maximum displacement at break s

Table 13.ITS maximum displacement at break s

	s (mm)				dev.st (-)			
	R	**E**	**P**	**B**	**R**	**E**	**P**	**B**
B	0.775	1.017	0.910	0.757	0.204	0.003	0.113	0.046
C	0.474	0.808	0.868	1.043	0.105	0.125	0.208	0.251
S	0.565	0.680	0.596	0.717	0.079	0.024	0.060	0.062

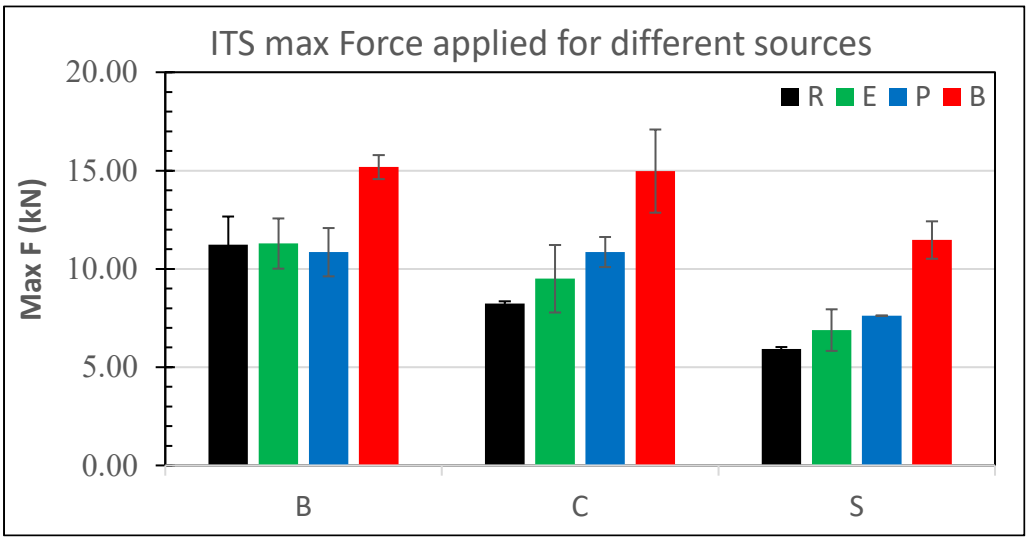

Figure 77. ITS peak load F

Table 14. ITS peak load F

	F (kN)				dev.st (-)			
	R	**E**	**P**	**B**	**R**	**E**	**P**	**B**
B	11.226	11.292	10.853	15.185	1.434	1.282	1.232	0.612
C	8.239	9.504	10.856	14.981	0.107	1.716	0.770	2.113
S	5.934	6.890	7.622	11.472	0.094	1.061	0.019	0.951

After the analysis of the results, the behaviour of each material is provided. First, BS had the lowest ITS values meaning that the binder has low tensile strength and does not glue with strong and sticky contact points the aggregates, showing the binder ageing that composes RA. Second, WS achieved the highest ITS values, evidencing a new and sticky binder covering and having stronger contact points between the aggregates. Moreover, it can be proven that even if the virgin binder is soft, it does not necessarily mean that it will have lower tensile strength, withstanding at 4ºC higher strains without fracturing.

Finally, RS shows an improved response, attributed to the enhancement of RA binder because of the implementation of the Rejuvenating Agents. It is clear that Rejuvenating Agents recover the rheology of the cortex, reduce the dynamic modulus softening the binder, and with ITS results is possible to analyze that it also increased the binder tensile strength upgrading RA mechanical properties.

As part of the analysis, the Ductility Toughness Index was also computed. It is calculated as the integral of the normalized curve in the post-peak region, considered to extend up to a strain of 2E-2 mm/mm from the peak. (Dalmazzo, Urbano, Riviera, & Santagata, Testing of reclaimed asphalt model systems for the evaluation of the effectiveness of rejuvenators, 2020). Figure 78 presents the results, where the potential increase of the ductility toughness index is evident by the addition of the Rejuvenating Agents, having an important action in the post-peak conditions. Nevertheless, the DTI is a parameter that should be investigated to characterize the chemicals' benefits better. The present work does not profoundly analyze the DTI because its performance corresponds to the post-peak region and requires a deeper investigation.

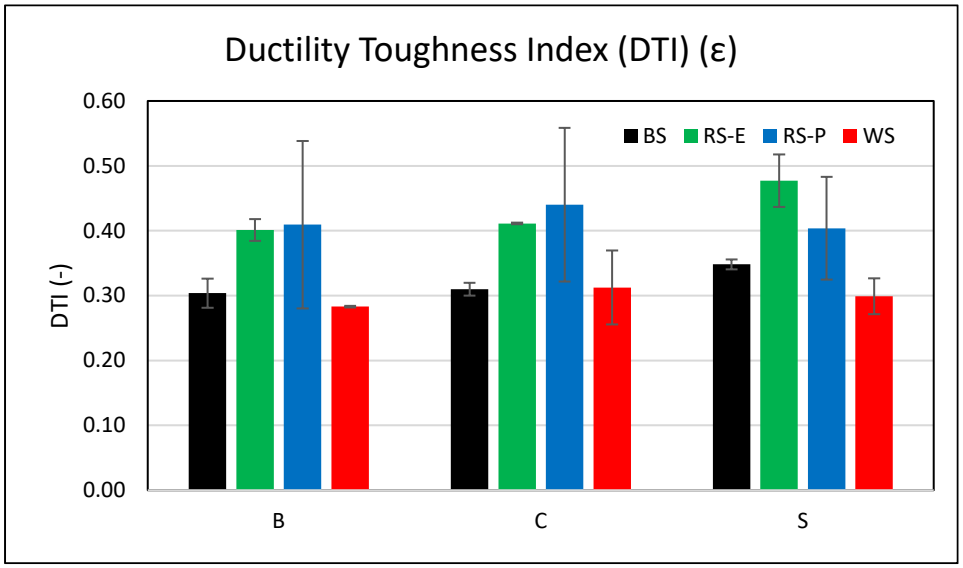

Figure 78. Ductility Toughness Index (DTI)

As a final analysis, the normalized values of ITS are evaluated versus the complex dynamic modulus (|E*|). The results are standardized concerning the reference conditions (WS) to characterize the equivalence to the ideal circumstances, rejuvenating RA until the mechanical properties equal WS. In this context, both ratios equal to 1 would be required to represent an ideal but impossible situation, creating two asymptotes. As it is clear that a perfect material would not be achieved from the recycling of RA, it was required to define the ranges where the results can be accepted. Following the accepting rule established for the dynamic modulus,

results between 1 and 1.2 are characterized by good stiffness behaviour. While for the ITS, it can be accepted results with at least 60% of WS tensile strength.

Three regions were defined as is shown in Figure 79: the areas are divided as optimum, fairly good and unacceptable. Furthermore, the material characterization is described for each of them.

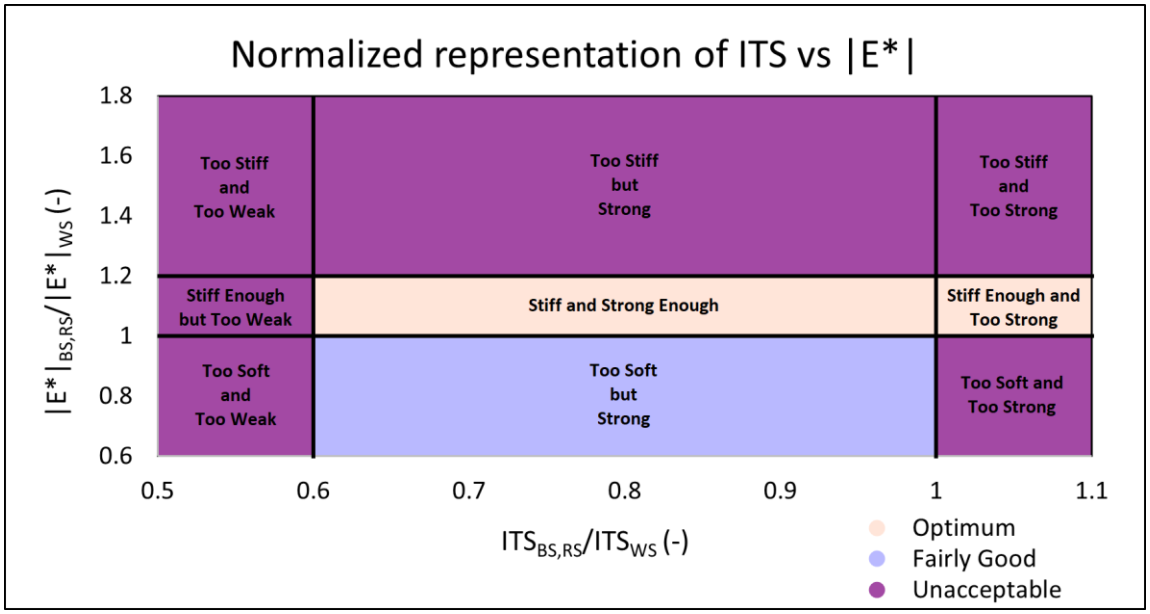

Figure 79. Zone definition for the normalized representation of ITS vs |E|*

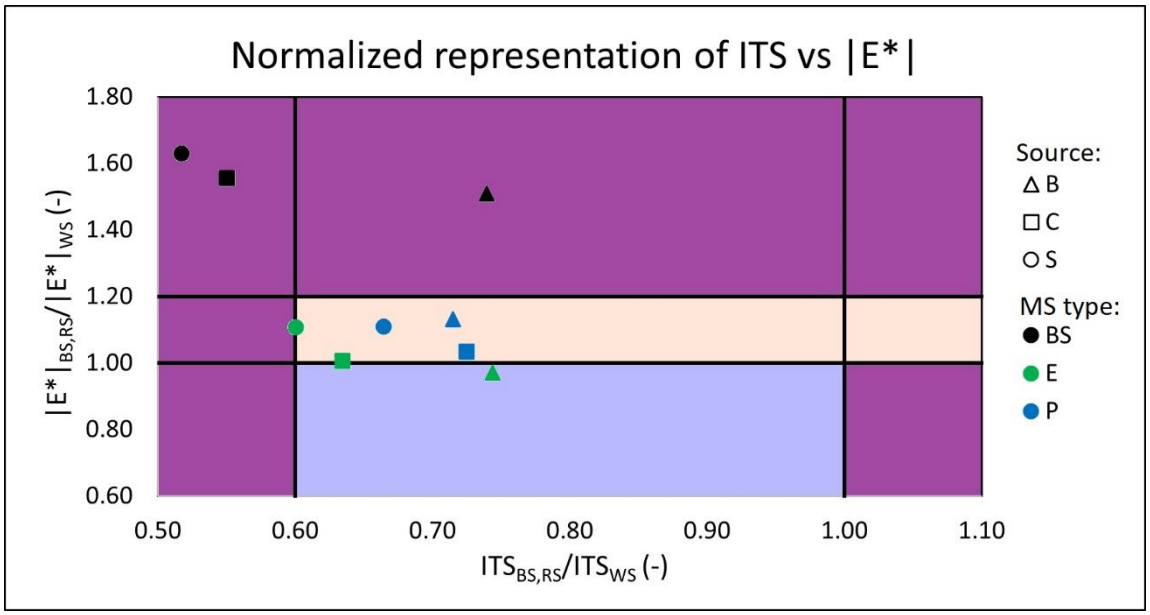

Figure 80. Normalized representation of ITS vs |E|*

Using the graph, the improvement of each RA source can be evidenced. For B, the Rejuvenating Agent enhanced the stiffness behaviour in terms of viscoelasticity, but the strength remains unaffected. On the other hand, C and S considerably improved both parameters, the stiffness and the strength, enhancing the mechanical properties of RA. The rejuvenated material will allow elastic deformations under load application and hold much more stress before it breaks.

6. CONCLUSIONS

This experimental study has validated the previous investigations on the Model System using three different RA sources, combined with two different Rejuvenating Agents, to assess the possible dependency of the rejuvenating effect on RA. Furthermore, MS aims to highlight the response of the rejuvenated binder phase by using a single-sized 5/8 RA material. Nevertheless, it must be highlighted that MS does not reproduce the mechanical behaviour of bituminous mixtures made up of 100% RA.

For each RA source, three different model systems were defined and designed to obtain a constant value of Voids in the Mineral Aggregate (VMA) equal to 30%, ensuring a constant lithic structure and similar contact points between aggregates. Therefore, the mechanical behaviour of MS depends mainly on the binder phase, limiting the effect of aggregates interlocking. RA sources evaluated were B, C and S. Regardless of RA source, three different MS were prepared: (i) a black system made with 100% 5/8 RA; (ii) a rejuvenated system composed of 5/8 RA mixed with a Rejuvenating Agent (E or P); (iii) a white system constituted by the aggregates extracted from RA mixed with 50/70 neat binder, keeping constant the percentage of the binder characteristic of each 5/8 RA source. Once the optimal dosage was defined considering the linear viscoelastic behaviour, the indirect tensile strength test was conducted to study low temperatures' performance.

By analyzing all the results acquired from the experimentation carried out, it emerged that:

1. From the compaction of BS sample, it was noticed higher the binder content is, higher the self-compaction and workability are. Also, the rotations to achieve the target height of the specimen are lower when the binder content increases. Therefore, the increase of

C1, k and the reduction of the number of rotations are related to the lubricant effects of the binder.

2. Also, it is evidenced that using the optimum dosage of the Rejuvenating Agents, the stiff binder is regenerated, and its viscosity is reduced: RS approach C1 values to the respective reference system (WS). Conversely, k is maintained constant even with the increasing Rejuvenating Agent dosage. This effect could be due to the greater compaction at the beginning, as obtained with C1, and a potential black rock effect in which part of RA is not rejuvenated and greater friction lowers the workability.
3. The master curves were a powerful tool to estimate the viscoelastic properties of each MS and define the optimum dosage of each Rejuvenating Agent. It was clear that dynamic modulus is affected by the ageing of the binder source, the coarser granulometry, bitumen and air voids content, and the dosage of the Rejuvenating Agent by weight of bitumen. The dynamic modulus values |E*| decrease as the dosage increases: this is because of the softening action of the Rejuvenating Agents on the stiff binder, changing the rheological characteristics. If its content is too low or too high does not regenerate the bitumen or exerts an exaggerated softening action, respectively. Furthermore, at lower temperatures, the overlapping of the curves is better than at high temperatures because the Rejuvenating Agent does not totally blend in the aged binder and some of the rejuvenated RA remain as black rocks.
4. The Rejuvenating Agent dosages selected as optimum were: 8% for B and S, while for C source, it was established for E 10.5% and P 14.5%. However, for C source were achieved values that are not economically feasible. Therefore, it must be considered the convenience of using or not this RA in future pavement constructions.

   Furthermore, it was analyzed that always Rejuvenating Agent E required a lower dosage than P. Using the optimum dosages, the master curves of RS overlapped WS for the

medium and low temperatures and the modulus ratio for BS and RS over WS was between 1 and 1.2.

5. BS and WS prepared with a constant VMA, similar lithic structure, but different binder content and percentage of air voids were tested in terms of dynamic modulus |E*| and elastic stiffness (ITSM) in indirect tensile configuration for all 5/8 RA sources. It was obtained that when the binder content is higher than 3.1%, ITSM can predict the moduli, obtaining results that correspond with the master curves obtained with the more advanced dynamic modulus test. For lower binder content, instead, the ITSM moduli were not comparable with dynamic modulus: The reason is that less force is required to generate the same elongation and the effect of solid skeleton. Therefore, it is established that the binder content is a limiting parameter for RA employed because of the different test configurations.
6. The ageing index of the binder phase computed as the ratio between BS and WS index compares how stiffer is the binder phase, respect to the reference conditions (WS). It is independent of the percentage of binder content and the lithic structure because these conditions are the same for all MS of each source. Another not considered parameter is the compaction degree, since the number of gyrations is close for each source. Therefore, if the ratio is equal to one, it will mean that the binder is not aged. The sources are organized as C, B, S in decreasing ageing index.
7. The ITSM and ITS tests are based on the indirect tensile configuration; their response mainly corresponds to the binder's mechanical properties. BS achieved the lowest ITS values because of the aged binder's poor strength. While the highest ITS values correspond to WS, evidencing a new and sticky binder covering and having stronger contact points between the aggregates. Moreover, the results proved that even if the virgin binder is soft, it does not necessarily mean that it will have lower tensile strength,

withstanding at 4ºC higher strains without fracturing. On the other hand, RS shows an improved response concerning BS. It is clear that Rejuvenating Agents recover the rheology of the cortex, reduce the dynamic modulus softening the binder, and with ITS results, a low increment of the binder tensile strength is obtained upgrading RA mechanical properties.

8. The normalized values of ITS evaluated graphed versus the complex dynamic modulus (|E*|) allowed to evidence RA improvements for each source. For B, the Rejuvenating Agent enhanced the stiffness behaviour in terms of viscoelasticity, but the strength remains unaffected. While, in C and S is markable the improvement of stiffness and strength, enhancing the mechanical properties of RA. The rejuvenated material will allow elastic deformations under load application and still return to its original shape. Also, it will hold much more stress before it breaks. For the defined ranges, it is concluded that all sources have improved their mechanical properties, being more evident in the reduction of stiffness than the strength increase.

The results highlighted the tangible effect of Rejuvenating Agents within the mixtures composed of RA. Indeed, from the various tests, significantly lower modulus and a reduced effect in stiffness values were obtained for regenerated samples confronting BS, evidencing the regeneration of the oxidized bitumen film covering RA.

As a conclusion is decided that Rejuvenating Agent P works better than E for the model system, but it must also be evaluated its behaviour in the mixture.

The proposed objectives were achieved. However, the experimentation of the model system needs to be developed extensively to obtain data resulting from different test methodologies and using several types of RA and Rejuvenating Agents.

7. BIBLIOGRAPHY

AASHTO T 378-17. (2019). *Determining the Dynamic Modulus and Flow Number for Asphalt Mixtures Using the Asphalt Mixture Performance Tester (AMPT)*. Washington, D.C.: American Association of State Highway and Transportation Officials.

AASHTO TP 107-18. (2019). *Determining the Damage Characteristic Curve and Failure Criterion Using the Asphalt Mixture Performance Tester (AMPT) Cyclic Fatigue Test*. Washington, D.C: American Association of State Highway and Transportation Officials.

Al-Qadi, I., Elseifi, M., & Carpenter, S. (2007, March). Reclaimed Asphalt Pavement – A Literature Review. Illinois.

Asphalt Institute. (2014). MS-2 Asphalt Mix Design Methods.

Dalmazzo, D., Urbano, L., Riviera, P. P., & Santagata, E. (2020). Testing of reclaimed asphalt model systems for the evaluation of the effectiveness of rejuvenators.

Dalmazzo, D., Urbano, L., Riviera, P. P., & Santagata, E. (2020). Testing of reclaimed asphalt model systems for the evaluation of the effectiveness of rejuvenators.

EN 1097-6. (2013). *Tests for mechanical and physical properties of aggregates Part 6: Determination of particle density and water absorption*. Brussels: European Committee for Standardization.

EN 1097-7. (2008). *Tests for mechanical and physical properties of aggregates Part 7: Determination of the particle density of filler-Pyknometer method*. Brussels: European Committee for Standardization.

EN 12697-2:2015+A1. (2019). *Bituminous mixtures — Test methods Part 2: Determination of particle size distribution*. Brussels: European Committee for Standardization.

EN 12697-23. (2017). *Bituminous mixtures - Test methods - Part 23: Determination of the indirect tensile strength of bituminous specimens*. Brussels: European Committee for Standardization.

EN 12697-26. (2018). *Bituminous mixtures - Test methods Part 26: Stiffness*. Brussels: European Committee for Standardization.

EN 12697-31. (2019). *Bituminous mixtures – Test methods Part 31: Specimen preparation by gyratory compactor*. Brussels: European Committee for Standardization.

EN 12697-5. (2018). *Bituminous mixtures - Test methods Part 5: Determination of the maximum density*. Brussels: European Committee for Standardization.

EN 12697-6. (2020). *Bituminous mixtures-Test methods - Part 6: Determination of bulk density of bituminous specimens*. Italia: UNI.

EN 13043:2013. (2013). *Aggregates for bituminous mixtures and surface treatments for roads, airfields and other trafficked areas*. Brussels: European Committee for Standardization.

EN 13108-8. (2016). *Bituminous mixtures - Material specifications - Part 8: Reclaimed Asphalt*. Brussels: European Committee for Standardization.

EN 933-1. (2012). *Tests for geometrical properties of aggregates - Part 1:Determination of particle size distribution - Sieving method*. Brussels: European Committee for Standardization.

EN12697-39. (2020). *Bituminous mixtures - Test methods - Part 39: Binder content by ignition*. Brussels: European Committee for Standardization.

Jamshidi, A., White, G., Hosseinpour, M., Kurumisawa, K., & Othman Hamzah, M. (2019). Characterization of effects of reclaimed asphalt pavement (RAP) source and content on

dynamic modulus of hot mix asphalt concrete. *Construction and building materials*, pp. 487-497.

Kendhal, P. S., & Mallick. (1997). Pavement Recycling Guidelines for State and Local – Participant's Reference Book, Report No. FHWA-SA-98-042. Auburn: National Center for Asphalt Technology.

Kim, Y. R. (2009). Complex modulus characterization of asphalt concrete. In Y. R. Kim, *Modeling of Asphalt Concrete.* New York: McGraw-Hill.

Martins Zaumanis, R. B. (2014). Influence of six rejuvenators on the performance properties of Reclaimed. *Construction and Building materials*, 538-550.

Moghaddam, T. B., & Baaj, H. (2016). The use of Rejuvenating Agents in production of recycled hot mix asphalt: A systematic review,. *Construction and Building Materials*, pp. 805-816.

VARGAS, J., & NEUMANN. (2016). Normas de Tierra : Ensayos de Tracción Indirecta. *terra Lyon 2016*. Retrieved from https://craterre.hypotheses.org/files/2018/05/TERRA-2016_Th-4_Art-133_Vargas-Neumann.pdf

ATTACHMENTS

Black curve results for Feedstock material

	Black curve		
	% Passing average		
Sieve	**B 10 RA 0/8**	**C 20 RA 0/14**	**S 10 RA 0/8**
(mm)	**(%)**	**(%)**	**(%)**
25	100	100	100
20	100	100	100
16	100	99	100
14	100	95	100
12.5	100	92	100
10	100	82	100
8	99	74	97
6.3	94	65	84
4	73	48	59
2	47	30	37
1	27	18	23
0.5	14	10	13
0.25	6	6	7
0.063	1	1	1

Black curve results for 5/8 material

	Black curve		
	% Passing average		
Sieve	**B**	**C**	**S**
(mm)	**(%)**	**(%)**	**(%)**
8.0	100	100	100
6.3	75	52	61
5.6	44	22	33

White curve for Feedstock material

	White curve		
	% Passing average		
Sieve	**B 10 RA 0/8**	**C 20 RA 0/14**	**S 10 RA 0/8**
(mm)	**(%)**	**(%)**	**(%)**
25	100	100	100
20	100	100	100
16	100	99	100
14	100	96	100
12.5	100	95	100
10	100	87	100
8	99	80	98
6.3	96	72	88
4	81	58	67
2	59	42	48
1	42	29	35
0.5	30	22	27
0.25	20	16	20
0.063	10	9	13

White curve for 5/8 material

	White curve		
	% Passing average		
Sieve	**B**	**C**	**S**
(mm)	**(%)**	**(%)**	**(%)**
8.0	100	100	100
6.3	85	72	74
5.6	64	48	53
5	31	25	25
4	18	16	16
2	13	13	13
1	11	10	12
0.5	8	9	10
0.25	6	7	8
0.125	4	5	7
0.063	2	4	6

Specimens characteristics (130 mm height and 100 mm diameter)

ID	n giri	k	C1	Mvgeo	MMVT	vgeo	Gsb	%BMix	Ps	VMA
(-)	(-)	(-)	(-)	(g/cm3)	(g/cm3)	(%)	(g/cm3)	(%)	(%)	(%)
RB-00-1	82	8.1	59.28	1.963	2.628	25.3	2.720	3.5	96.5	30.3
RB-00-2	101	7.6	59.58	1.966	2.628	25.2	2.720	3.5	96.5	30.2
BB-00-1	114	7.5	61.10	1.976	2.579	23.4	2.720	3.5	96.5	29.9
BB-00-2	101	7.8	61.02	1.975	2.579	23.4	2.720	3.5	96.5	29.9
BB-00-3	123	7.4	61.21	1.971	2.579	23.6	2.720	3.5	96.5	30.0
RB-E8-1	69	7.4	61.82	1.962	2.620	25.1	2.720	3.5	96.2	30.6
RB-E8-2	87	7.6	60.82	1.963	2.620	25.1	2.720	3.5	96.2	30.5
RB-E8-3	102	7.2	61.24	1.972	2.620	24.8	2.720	3.5	96.2	30.2
RB-E8-4	107	7.6	60.07	1.960	2.620	25.2	2.720	3.5	96.2	30.6
RB-P8-1	73	7.9	60.66	1.957	2.622	25.4	2.720	3.5	96.2	30.8
RB-P8-2	80	7.8	60.77	1.964	2.622	25.1	2.720	3.5	96.2	30.5
RB-P8-3	82	7.9	60.37	1.963	2.622	25.1	2.720	3.5	96.2	30.6
RB-P8-4	111	7.5	60.15	1.962	2.622	25.2	2.720	3.5	96.2	30.6
RC-00-1	125	7.6	59.38	2.011	2.669	24.6	2.778	3.1	96.9	29.9
RC-00-2	177	7.4	58.92	2.014	2.669	24.5	2.778	3.1	96.9	29.8
BC-00-1	149	7.2	60.96	2.013	2.624	23.3	2.778	3.1	96.9	29.8
BC-00-2	98	6.9	63.12	2.017	2.624	23.1	2.778	3.1	96.9	29.7
BC-00-3	178	7.3	60.43	2.017	2.624	23.1	2.778	3.1	96.9	29.7
RC-E8-01	131	7.2	60.95	2.008	2.655	24.4	2.778	3.1	96.6	30.1
RC-E8-02	174	7.2	60.16	2.013	2.655	24.2	2.778	3.1	96.6	30.0
RC-P8-01	114	7.6	60.61	2.011	2.657	24.3	2.778	3.1	96.6	30.1
RC-P8-02	151	7.4	60.04	1.968	2.657	25.9	2.778	3.1	96.6	31.5
RC-E17.3-01	25	9.2	63.84	2.023	2.639	23.3	2.778	3.1	96.3	29.8
RC-E17.3-02	126	7.5	61.08	2.018	2.639	23.5	2.778	3.1	96.3	30.0
RC-P19.2-01	115	7.4	61.37	2.006	2.641	24.1	2.778	3.1	96.3	30.5
RC-P19.2-02	115	7.5	61.43	2.013	2.641	23.8	2.778	3.1	96.3	30.2
RC-E10.5-01	146	7.5	60.71	2.018	2.631	23.3	2.778	3.1	96.5	29.9
RC-E10.5-02	146	7.7	60.45	2.016	2.631	23.4	2.778	3.1	96.5	29.9
RC-E10.5-03	142	7.4	61.08	2.015	2.631	23.4	2.778	3.1	96.5	30.0
RC-P14.5-01	102	7.8	61.17	2.014	2.642	23.8	2.778	3.1	96.4	30.1
RC-P14.5-02	130	7.7	60.21	2.018	2.642	23.6	2.778	3.1	96.4	29.9
RC-P14.5-03	147	7.4	60.76	2.010	2.642	23.9	2.778	3.1	96.4	30.2
RS-00-1	183	6.6	58.29	1.939	2.664	27.2	2.727	2.8	97.2	30.9
RS-00-2	205	6.5	58.40	1.940	2.664	27.1	2.727	2.8	97.2	30.8
BS-00-1	251	6.1	59.92	1.923	2.626	26.8	2.727	2.8	97.2	31.4
BS-00-2	251	5.8	60.36	1.928	2.626	26.6	2.727	2.8	97.2	31.3
BS-00-3	208	6.6	59.38	1.953	2.626	25.6	2.727	2.8	97.2	30.4
RS-E8-01	214	6.3	59.57	1.940	2.647	26.7	2.727	2.8	97.0	31.0
RS-E8-02	200	6.3	59.73	1.946	2.647	26.5	2.727	2.8	97.0	30.8
RS-E8-03	244	6.3	59.41	1.955	2.647	26.1	2.727	2.8	97.0	30.4
RS-E8-04	276	6.2	59.37	1.953	2.647	26.2	2.727	2.8	97.0	30.5
RS-P8-01	150	6.5	60.24	1.950	2.648	26.4	2.727	2.7	97.0	30.6
RS-P8-02	186	6.3	60.19	1.959	2.648	26.0	2.727	2.7	97.0	30.3
RS-P8-03	201	6.3	59.65	1.950	2.648	26.3	2.727	2.8	97.0	30.6
RS-P8-04	155	6.3	60.40	1.950	2.648	26.3	2.727	2.8	97.0	30.6

Specimens characteristics (65 mm height and 100 mm diameter)

ID	n giri	k	C1	Mv_{geo}	MMVT	v_{geo}	Gsb	$\%B_{Mix}$	Ps	VMA
(-)	(-)	(-)	(-)	(g/cm3)	(g/cm3)	(%)	(g/cm3)	(%)	(%)	(%)
RB-00-1	136	7.3	60.5	1.999	2.628	23.9	2.720	3.5	96.5	29.1
RB-00-2	93	7.4	60.4	1.960	2.628	25.4	2.720	3.5	96.5	30.5
BB-00-1	85	7.6	61.8	1.959	2.579	24.1	2.720	3.5	96.5	30.5
BB-00-2	182	6.5	61.8	1.966	2.579	23.8	2.720	3.5	96.5	30.2
RB-E8-1	122	6.23	62.6	1.963	2.620	25.1	2.720	3.5	96.2	30.5
RB-E8-2	208	6.17	61.6	1.963	2.620	25.1	2.720	3.5	96.2	30.5
RB-P8-1	87	7.04	62.3	1.965	2.622	25.1	2.720	3.5	96.2	30.5
RB-P8-2	178	6.78	60.5	1.968	2.622	24.9	2.720	3.5	96.2	30.4
RC-00-1	119	6.9	61.0	2.001	2.669	25.0	2.778	3.1	96.9	30.2
RC-00-2	177	7.3	59.3	2.001	2.669	25.0	2.778	3.1	96.9	30.2
BC-00-1	203	5.9	62.7	1.990	2.624	24.2	2.778	3.1	96.9	30.6
BC-00-2	141	7.0	61.8	2.010	2.624	23.4	2.778	3.1	96.9	29.9
RC-E10.5-01	321	6.5	61.0	2.010	2.631	23.6	2.778	3.1	96.5	30.1
RC-E10.5-02	138	7.2	61.7	2.002	2.631	23.9	2.778	3.1	96.5	30.4
RC-P14.5-01	143	7.0	61.7	2.002	2.642	24.2	2.778	3.1	96.4	30.5
RC-P14.5-02	186	6.9	61.4	2.017	2.642	23.7	2.778	3.1	96.4	30.0
RS-00-1	189	***	***	1.934	2.664	27.4	2.727	2.8	97.2	31.0
RS-00-2	251	5.9	59.7	1.932	2.664	27.5	2.727	2.8	97.2	31.1
BS-00-1	227	5.5	61.5	1.919	2.626	26.9	2.727	2.8	97.2	31.6
BS-00-2	163	5.8	61.7	1.932	2.626	26.4	2.727	2.8	97.2	31.1
RS-E8-01	251	5.6	60.1	1.924	2.647	27.3	2.727	2.8	97.0	31.5
RS-E8-02	219	6.2	60.2	1.946	2.647	26.5	2.727	2.8	97.0	30.8
RS-P8-01	268	5.4	61.4	1.961	2.648	25.9	2.727	2.7	97.0	30.2
RS-P8-02	321	5.7	59.7	1.935	2.648	26.9	2.727	2.8	97.0	31.2

C1 evaluation for B source with different Rejuvenating Agent dosages.

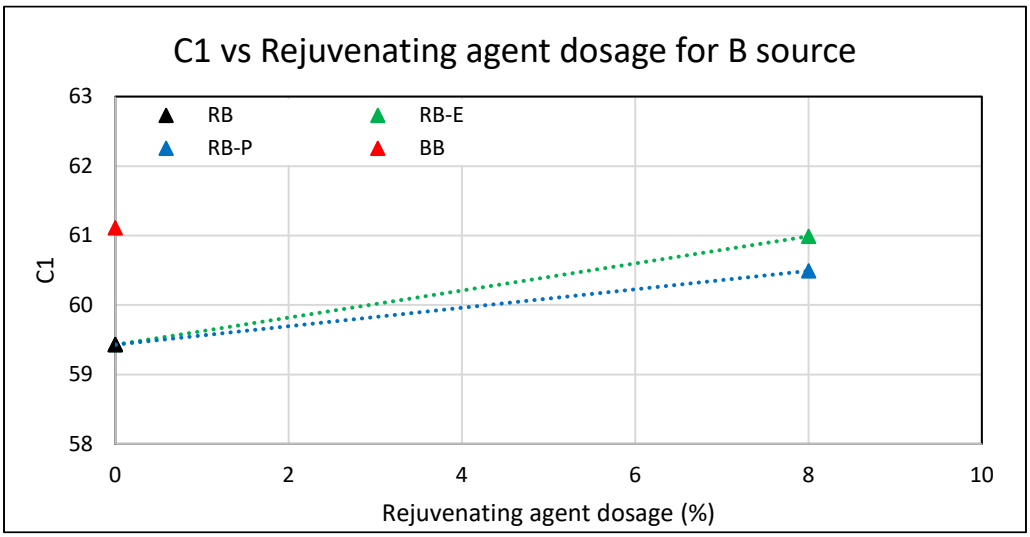

C1 evaluation for C source with different Rejuvenating Agent dosages.

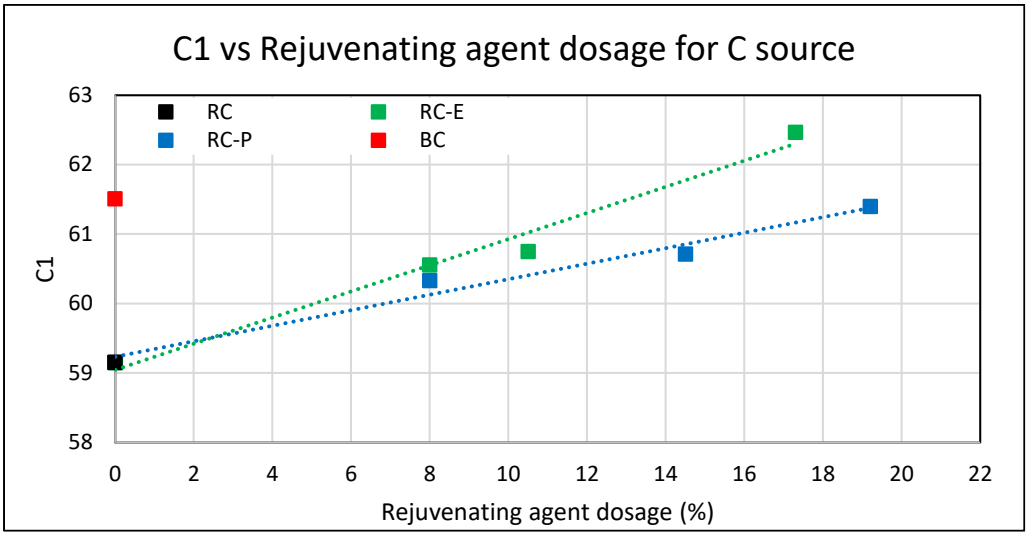

C1 evaluation for S source with different Rejuvenating Agent dosages.

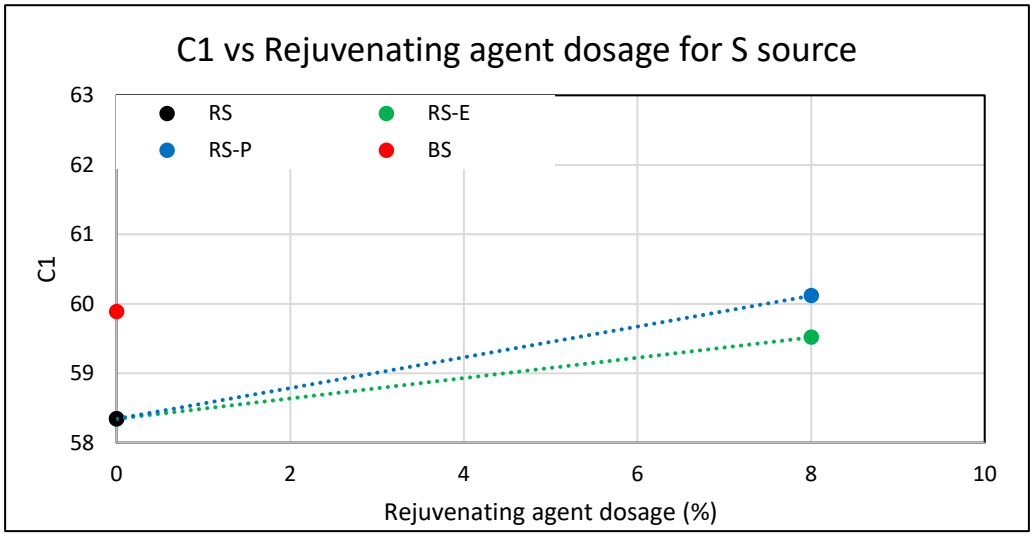

k evaluation for B source with different Rejuvenating Agent dosages.

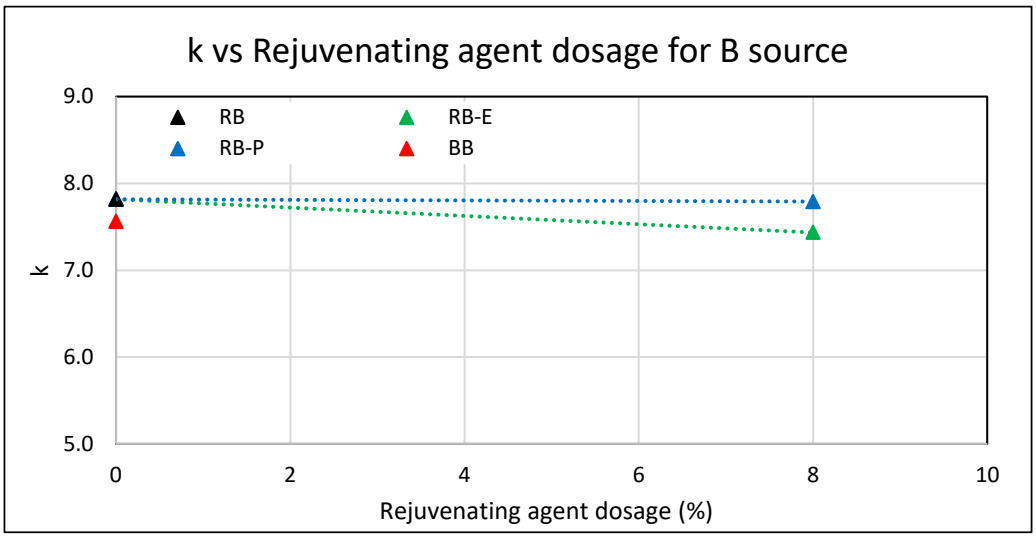

k evaluation for C source with different Rejuvenating Agent dosages.

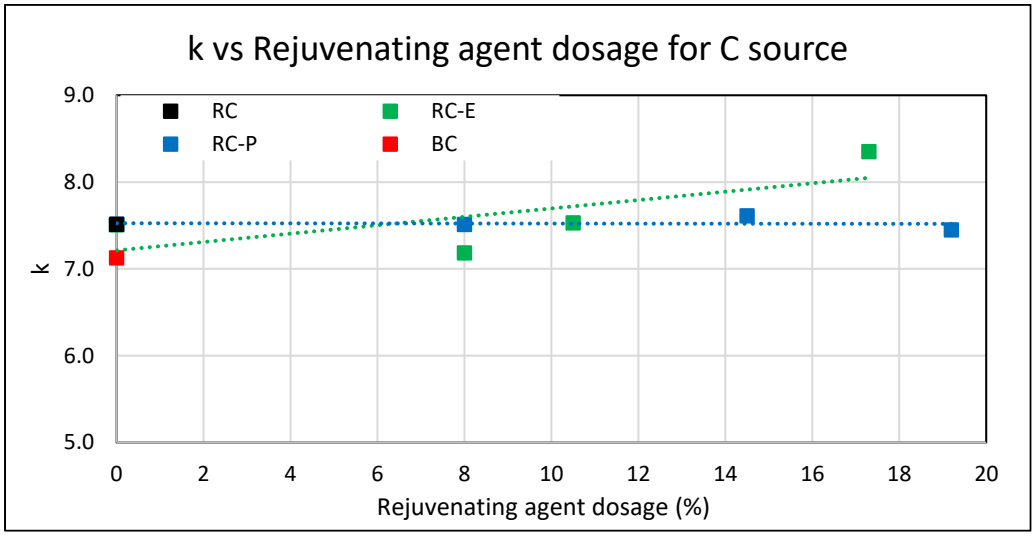

k evaluation for S source with different Rejuvenating Agent dosages.

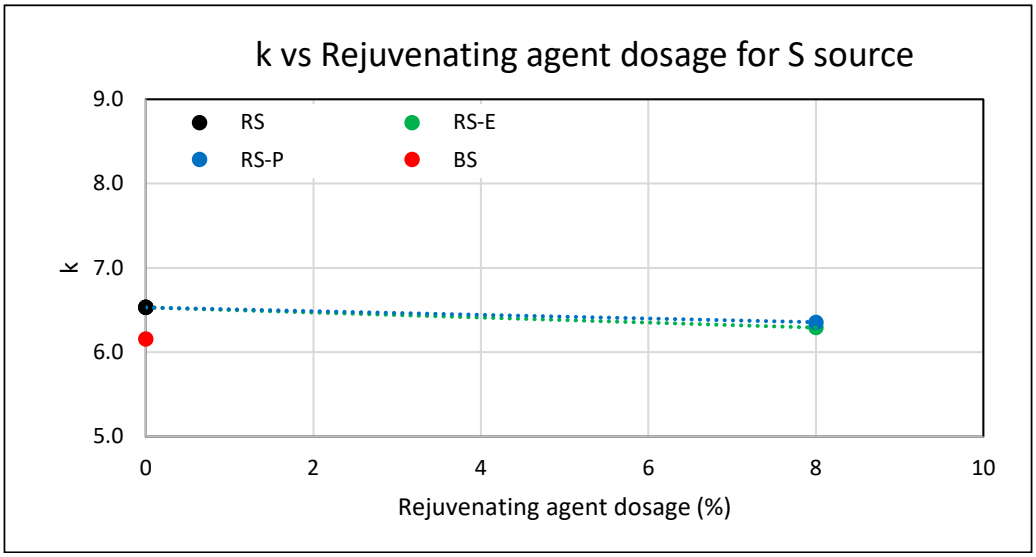

ACKNOWLEDGMENT

I want to thank God for so many blessings and opportunities, to my parents for always believing in me, in my abilities and discipline, for supporting me at all times, and for letting me know that I am capable. It has not been easy being away from home for the last two years, but all the sacrifices were worth it. I am too grateful to all the people who stood with me during this process, for their teachings and also at the time for the words of encouragement, Andrea, Tatiana, Daniel, Brenda, Vanessa and Paolo; I will never forget how loved they made me feel. I am pretty sure that this path would not be the same without them.

Last but not least, I would like to express my genuine gratitude to my advisors Prof. Ezio Santagata, Prof. Davide Dalmazzo, Prof. Pier Paolo Riviera, for the trust and guidance during the thesis work, and specially Ing. Leonardo Urbano, I will always be thankful for your help, patience, and shared knowledge.

Gracias, Javeriana Cali por ofrecerme la oportunidad de vivir este proceso educativo y sus desafíos.

Grazie Politecnico di Torino per tutta la conoscenza, gli amici e le esperienze.

Carolina Gil Botero